

General variational many-body theory with complete self-consistency for trapped bosonic systems

Alexej I. Streltsov*, Ofir E. Alon†, and Lorenz S. Cederbaum‡

Theoretische Chemie, Universität Heidelberg, D-69120 Heidelberg, Germany

(Dated: June 25, 2018)

* E-mail: alexej@tc.pci.uni-heidelberg.de

† E-mail: ofir@tc.pci.uni-heidelberg.de

‡ E-mail: Lorenz.Cederbaum@urz.uni-heidelberg.de

Abstract

In this work we develop a complete variational many-body theory for a system of N trapped bosons interacting via a general two-body potential. The many-body solution of this system is expanded over orthogonal many-body basis functions (configurations). In this theory both the many-body basis functions *and* the respective expansion coefficients are treated as variational parameters. The optimal variational parameters are obtained *self-consistently* by solving a coupled system of non-eigenvalue – generally integro-differential – equations to get the one-particle functions and by diagonalizing the secular matrix problem to find the expansion coefficients. We call this theory multi-configurational Hartree for bosons or MCHB(M), where M specifies explicitly the number of one-particle functions used to construct the configurations. General rules for evaluating the matrix elements of one- and two-particle operators are derived and applied to construct the secular Hamiltonian matrix. We discuss properties of the derived equations. We show that in the limiting cases of one configuration the theory boils down to the well-known Gross-Pitaevskii and the recently developed multi-orbital mean-fields. The invariance of the complete solution with respect to unitary transformations of the one-particle functions is utilized to find the solution with the minimal number of contributing configurations.

In the second part of our work we implement and apply the developed theory. It is demonstrated that for any practical computation where the configurational space is restricted, the description of trapped bosonic systems strongly depends on the choice of the many-body basis set used, i.e., self-consistency is of great relevance. As illustrative examples we consider bosonic systems trapped in one- and two-dimensional symmetric and asymmetric double-well potentials. We demonstrate that self-consistency has great impact on the predicted physical properties of the ground and excited states and show that the lack of self-consistency may lead to physically wrong predictions. The convergence of the general MCHB(M) scheme with a growing number M is validated in a specific case of two bosons trapped in a symmetric double-well.

PACS numbers: 03.75.Hh,03.65.Ge,03.75.Nt

I. INTRODUCTION

The first experimental realizations of Bose-Einstein condensation in trapped ultra-cold atomic clouds [1, 2, 3] renewed a great interest in the experimental and theoretical descriptions of this phenomenon. Modern experimental setups utilize magnetic [4], electric [5] and optical dipole fields [6] or their combinations to control the trapping and guiding of the ultra-cold atoms. The number of condensed atoms in these experiments varies from several dozens [7] to several millions [1, 2, 3]. Magnetically-tunable Feshbach resonances [8] make it possible to control the strength and sign of the inter-particle interactions. All these experimental tools may be used to design a bosonic system [9, 10, 11] and to study its time-independent and time-dependent properties.

From the theoretical point of view we have to study the properties of the collection of interacting many-electron atoms immersed in a time-dependent crossing electric and magnetic fields. This very complicated quantum mechanical many-body problem is replaced usually by a model Hamiltonian [12, 13, 14, 15]. Typically, the diluteness of the atomic cloud allows to consider the atoms as point-like particles with pairwise interaction and to neglect three-body and higher order collisions. The crossing electric and magnetic fields are replaced by an effective external trap potential. Within these assumptions the original system is modelled as a collection of massive point-like particles interacting via repulsive or attractive pairwise inter-particle interaction immersed in an external trap potential of known geometry.

However, there are only a few examples of the model many-body Hamiltonians the exact solutions of which are known, see, e.g., Refs. [16, 17, 18] and references therein. For general inter-particle interactions and trap geometries the problem can be attacked only within the framework of approximate and numerical methods. The most popular one is the variational approach, where the form or a specific ansatz of the trial many-body function is postulated. This ansatz depends on several parameters, and to solve the problem means to find the optimal set of the parameters which would minimize the expectation value of the Hamiltonian. Clearly, the more parameters are involved the closer the obtained solution to the exact true many-body function is.

One of the widely and successfully used approximations is the Gross-Pitaevskii (GP) ansatz [19], where it is assumed that each boson resides in a single spatial function, i.e.,

the many-body bosonic solution is presented as a product of identical one-particle functions (GP orbital):

$$\Psi(\vec{r}_1, \vec{r}_2, \dots, \vec{r}_N) = \varphi(\vec{r}_1)\varphi(\vec{r}_2) \cdots \varphi(\vec{r}_N). \quad (1)$$

This ansatz has only one variational parameter - the shape of the GP orbital φ . Orbitals with different shapes give different approximations to the true many-body solution. The "optimal" orbital is obtained by minimizing the expectation value of the Hamiltonian with respect to φ , which is equivalent to solving the very known GP equation. The GP solution is *self-consistent*, i.e., the shape of the GP orbital depends on the number of bosons and strength of the inter-particle interaction in addition to the geometry of the external trap potential. However, despite the great success of the GP ansatz, see Refs.[12, 13, 14, 15] and references therein, there are ample physical situations this one-orbital mean-field theory cannot describe, such as the depletion and fragmentation of trapped condensates and appearance of Mott-insulator phases of cold bosonic atoms in optical lattices. The natural way to resolve these difficulties is to take a more general many-body ansatz and to go, therefore, beyond Gross-Pitaevskii theory.

Recently, a more general mean-field theory for bosons has been put forward [20, 21, 22]. The multi-orbital, or best mean-field (BMF) theory as it is also called has been derived by considering the many-body ansatz where n_1 bosons reside in one orbital ϕ_1 , n_2 bosons in a second orbital ϕ_2 and so on:

$$\Psi(\vec{r}_1, \dots, \vec{r}_N) = \hat{\mathcal{S}}\phi_1(\vec{r}_1) \cdots \phi_1(\vec{r}_{n_1})\phi_2(\vec{r}_{n_1+1}) \cdots \phi_2(\vec{r}_{n_1+n_2}) \cdots \phi_M(\vec{r}_{n_1+n_2+\dots+n_M}), \quad (2)$$

where $\hat{\mathcal{S}}$ is the symmetrizing operator required for bosons. In the multi-orbital mean-field theory the shapes of the one-particle functions ϕ_i , the occupation numbers n_i as well as the number M of one-particle functions are considered as variational parameters. The optimal parameters of this many-body function are obtained by solving a respective system of coupled non-linear equations. The resulting mean-field solution is also *self-consistent*, and depends on the number of bosons and strength of the inter-particle interaction in addition to the geometry of the external trap potential. The BMF theory was used, among several applications and predictions, to show [23] that with increasing inter-particle interaction, the ground state of a trapped bosonic system on its pathway from condensation towards fermionization, gradually passes through two-, three- and up to M -fold stages of the fragmentation. The multi-orbital mean-field theory, when applied to the optical lattices, predicts [24] the

transition from the super-fluid to the Mott-insulator phase and reveals a variety of new Mott-Insulator phases.

The self-consistent GP and BMF theories considered above successfully describe the main features of the condensation, fragmentation and fermionization phenomena. However, the mean-field ansatzes used are made of only one many-body function of known type (a permanent) and are, therefore, incapable – by construction – to describe the depletion and fluctuations of the many-body states. To improve the many-body description further it is natural to go beyond mean-fields and take as an ansatz a linear combination of several *known* N-body basis functions:

$$|\Psi\rangle = \sum_i C_i |\Phi_i\rangle, \quad (3)$$

where $\{|\Phi_i\rangle\}$ is a set of N-body basis functions and $\{C_i\}$ are the expansion coefficients. In quantum chemistry, Eq.(3) is called *configuration interaction* (CI) expansion [25], because every many-body basis function (*configuration*) is attributed to a simple physical situation. For bosonic systems, a configuration may represent a condensate, i.e., the state where all bosons reside in the same orbital, an excited state where $N - i$ bosons remain condensed and i bosons are excited out of a condensate, a two-fold fragmented state where a macroscopic number of bosons n_1 reside in one orbital and $n_2 = N - n_1$ bosons in another, and so on. The variational problem of finding the unknown expansion coefficients C_i in this case is reduced to the diagonalization of the respective secular Hamiltonian matrix [25]. This method is also known as exact diagonalization technique, because if all possible configurations are considered, i.e., the N-body basis is *complete*, then this expansion is *exact*, irrespective to the particular choice of the many-body basis functions $\{|\Phi_i\rangle\}$. However, the secular Hamiltonian matrix in this case is an infinite matrix.

To make real computations tractable, the number of configurations in the expansion Eq.(3), of course, has to be truncated. The configurational space in this case spans a restricted subspace of the Hilbert space. The exact diagonalization studies within truncated configurational spaces have been used to provide a many-body description of repulsive and attractive condensates, see, e.g., Refs.[26, 27, 28]. In these investigations, many-body basis functions comprised of *a priori fixed orbitals* have been utilized to study the properties of the bosonic system as a function of the inter-particle interaction strength. However, it is clear that exact diagonalizations performed within different truncations of the CI expansion will

give different results. Moreover, truncated CI expansions of the same size but utilizing different sets of orbitals will also give different results in general. Indeed, it was demonstrated [27, 29] that the total energy obtained by the exact diagonalization in a restricted configurational space can sometimes be even worse than the self-consistent GP mean-field energy. In these cases we encounter the situation that due to the implemented self-consistency, a single mean-field function provides a better description than a very large fixed-orbital many-body CI expansion.

A question addressed in this work is how the choice of the many-body basis functions impacts the results obtained within a restricted configurational space. By comparing the many-body results obtained within different basis sets we can find the energetically most favorable one, i.e., the best many-body basis set. The main goal of the present investigation is to formulate a many-body theory which would provide the best set of many-body basis functions in a desired, i.e., truncated, subspace of the Hilbert space. To achieve this goal, we apply a *general* variational principle where we treat *both* the set of many-body basis functions $\{|\Phi_i\rangle\}$ and the set of the expansion coefficients $\{C_i\}$ appearing in the expansion Eq.(3) as variational parameters which are to be optimized. This results, as we shall see below, in a many-body theory for bosonic systems with complete self-consistency, which we refer to as Multi-Configurational Hartree for Bosons or MCHB(M), where M specifies explicitly the number of one-particle functions used to construct the configurations.

Some hints that self-consistency is useful and important in attacking the many-boson problem *beyond* mean-field have already been addressed in the literature in the context of symmetric double-well potentials and two-orbital configuration-interaction expansions. Spekkens and Sipe [30] provide an approximative analytic as well as numerical solutions for the bosonic system trapped in symmetric double-well potentials in the regime where the inter-particle interaction can be treated perturbatively. More recently, Reinhard [31] and coworkers have combined a partial nonlinear optimization of the many-body basis functions with a linear variational principle for the expansion coefficients to describe ground and excited states of bosons trapped in a symmetric double-well. Here, we would like to stress that the many-body variational theory which we develop in this paper is *complete*, because we fully optimize all expansion coefficients as well as all the many-body basis functions appearing in the expansion Eq.(3), and *general* because it is valid for any trap geometry, for any physical shape of the inter-particle interaction and in any dimension.

The structure of the paper is as follows. In Sec.II A, a trapped N-bosonic system interacting via a general pairwise potential is considered. The multi-configurational expansion Eq.(3) is used as an ansatz for the true many-body wave function of this system. The variational principle is used in Sec.II B to formulate the general equations which allow one to find the best many-body basis functions and the corresponding expansion coefficients self-consistently in the desired active space. Sec.II B 1 is devoted to the problem of finding the expansion coefficients. In this section we provide the general rules for evaluating matrix elements of one- and two-body operators between two general basis functions (permanents) and apply them to construct the secular Hamiltonian matrix. The problem of finding the optimal basis functions is considered in Sec.II B 2, where the working equations for the general case are derived in closed form using the elements of the reduced one- and two-body density matrices. Properties of the resulting equations are discussed in Sec.II C. In particular, we demonstrate that in the limiting cases of a single permanent, the derived equations boil down to the one-orbital Gross-Pitaevskii and multi-orbital mean-fields equations. Sec.III A opens the second part of our work and provides explicitly the working equations of MCHB(2), i.e., the case where the basis functions are obtained as all possible permutations of N bosons over two orbitals. As an inter-particle potential we implement the popular contact interaction. The formalism is used to investigate the impact of self-consistency on many-body predictions. The ground state of N=1000 bosons trapped in a symmetric one-dimensional double-well trap is investigated in Sec.III B and for an asymmetric one in Sec.III C. In Sec.III D we show for these examples that the number of many-body basis functions contributing to the expansion in Eq.(3) can be significantly reduced by appropriately choosing the orbitals used to construct the many-body basis functions. Excited states of the bosonic system trapped in a symmetric double-well trap are investigated in Sec.III E. The two-dimensional bosonic system trapped in symmetric double-well is studied in Sec.III F. The convergence of the MCHB(M) theory is addressed in Sec.IV where we apply different levels $M= 2, \dots, 10$ of MCHB(M) theory to study ground state properties of two bosons trapped in a symmetric double-well trap. Finally, Sec.V summarizes our results and conclusions.

II. THEORY

A. Preliminaries

Consider a system of N identical spinless bosons of mass m immersed in an external time-independent trap potential $V(\vec{r})$ and interacting via a general pairwise interaction potential $W(\vec{r}_i - \vec{r}_j)$ where \vec{r}_i is the position of the i -th particle. By using bosonic annihilation and creation operators b_i and b_j^\dagger , $b_i b_j^\dagger - b_j^\dagger b_i = \delta_{ij}$ which are associated with a given set of orbitals $\{\phi_i\}$, the Hamiltonian of the system takes on the standard form in second quantization language:

$$\hat{H} = \hat{h} + \hat{W}$$

$$\hat{h} = \sum_{i,j=1} h_{ij} b_i^\dagger b_j \quad , \quad \hat{W} = \frac{1}{2} \sum_{i,j,k,l=1} W_{ijkl} b_i^\dagger b_j^\dagger b_l b_k, \quad (4)$$

where the one- and two-body matrix elements read

$$h_{ij} = \int \phi_i^*(\vec{r}) \left(-\frac{\hbar^2}{2m} \nabla_{\vec{r}}^2 + V(\vec{r}) \right) \phi_j(\vec{r}) d\vec{r} \quad (5)$$

and

$$W_{ijkl} = \int \int \phi_i^*(\vec{r}) \phi_j^*(\vec{r}') W(\vec{r} - \vec{r}') \phi_k(\vec{r}) \phi_l(\vec{r}') d\vec{r} d\vec{r}'. \quad (6)$$

Our general intention is to find time-independent solutions of this Hamiltonian in a form of expansion (3) over basis functions. Every basis function being a many-body function must depend on the coordinates of all N bosons. The simplest way to construct it is to take a product of different orthogonal orbitals, so called Hartree product $\Phi_i \equiv \Phi_i(\vec{r}_1, \vec{r}_2, \dots, \vec{r}_N) = \hat{S} \phi_1(\vec{r}_1) \phi_2(\vec{r}_2) \cdots \phi_N(\vec{r}_N)$, and to apply the symmetrizing operator \hat{S} to fulfil the Bose statistic. When all the orbitals are identical, we obtain a GP-like many-body basis function (see Eq.(1)) used to describe condensation. If some fraction of bosons resides in one orbital and the rest in another one, we deal with a basis function describing two-fold fragmentation, and so on. The general many-body basis function can be considered as one of the configurations resulting due to permutation of N bosons over M orbitals. In second quantization language this general many-body function, also known as permanent, reads

$$\Phi_i(\vec{r}_1, \vec{r}_2, \dots, \vec{r}_N) = \frac{1}{\sqrt{n_1! n_2! n_3! \cdots n_M!}} (b_1^\dagger)^{n_1} (b_2^\dagger)^{n_2} \cdots (b_M^\dagger)^{n_M} |vac\rangle = |n_1, n_2, n_3, \dots, n_M\rangle \quad (7)$$

where M is a number of the one-particle functions, $n_1 + n_2 + n_3 + \dots + n_M = N$, and $|vac\rangle$ is the vacuum.

We recall that if the many-body basis set $|\Phi_i\rangle$ in expansion (3) is *complete*, i.e., it spans the whole N -boson Hilbert space, then expansion (3) is exact irrespective to the particular choice of the basis functions used. In the present formulation, this is achieved when the number of the one-particle functions $M \rightarrow \infty$. However, to make real computations tractable the size of the expansion (3) and hence the number of the one-particle basis functions M has to be restricted. Let us assume that the many-body basis set $\{|\Phi_i\rangle\}$ is formed by *all* possible configurations appearing as permutation of N bosons over M orbitals. The total number of configurations, and therefore the size of the expansion in this case is $\binom{M+N-1}{N}$. For example, for a system of $N=1000$ bosons and $M=3$ orbitals the total number of configurations is 501,501 while for $M=4$, the number of configurations is already 167,668,501, which would make practical computations impossible. Another consequence of the truncation is that different sets of orbitals used to construct many-body basis sets of the same size would lead to different approximations to the exact many-body Ψ . As truncated CI expansions become very demanding with increasing N and/or M , it is of great advantage to exploit this property. Namely, it is desirable to find not only expansion coefficients but also the "best" set of one-particle basis functions. Combined together, these lead to the self-consistent optimal CI expansion. To fulfil this goal, we apply in this work the variational principle, which defines the energetically most favorable solution as the best one.

B. The general variational approach

Let us consider a system of N bosons and restrict the number of one-particle functions to M . Then, the trial many-body function (expansion (3)) takes on the following form:

$$|\Psi\rangle = \sum_{n_1, n_2, \dots, n_M} C_{(n_1, n_2, n_3, \dots, n_M)} |n_1, n_2, n_3, \dots, n_M\rangle \equiv \sum_{\vec{n}} C_{\vec{n}} |\vec{n}\rangle, \quad (8)$$

where n_1, n_2, \dots, n_M are the number of bosons residing in orbitals $\phi_1, \phi_2, \dots, \phi_M$. The summation runs over all possible configurations $\vec{n} = (n_1, n_2, n_3, \dots, n_M)$, preserving total number of particles $n_1 + n_2 + \dots + n_M = N$. The expectation value of the Hamiltonian evaluated

with this trial function reads:

$$\langle \Psi | \hat{H} | \Psi \rangle = \sum_{\vec{n}, \vec{n}'} C_{\vec{n}}^* C_{\vec{n}'} \langle \vec{n} | \hat{H} | \vec{n}' \rangle. \quad (9)$$

This expression depends on two types of variational parameters: on the expansion coefficients $\{C_{\vec{n}} \equiv C_{(n_1, n_2, n_3, \dots, n_M)}\}$ and on the particular choice of the one-particle functions $\phi_1, \phi_2, \dots, \phi_M \equiv \{\phi_i\}$. Our main goal is to find the values of these parameters for which $\langle \Psi | \hat{H} | \Psi \rangle$ is a minimum. The natural requirements on normalization of the trial many-body function $\langle \Psi | \Psi \rangle = 1$ and orthonormalization of all the one-particle functions $\langle \phi_i | \phi_j \rangle = \delta_{ij}$ allow us to formulate the minimization problem within Lagrange's method of undetermined multipliers. Here we have to stress that these are the only constraints applied.

The Lagrange energy functional takes on the form:

$$\mathcal{L}[\{C_{\vec{n}}\}, \{\phi_i\}] = \langle \Psi | \hat{H} | \Psi \rangle + \mathcal{E}(1 - \sum_{\vec{n}} C_{\vec{n}}^* C_{\vec{n}}) + \sum_{i=1}^M \sum_{j=1}^M \mu_{ij}(\delta_{ij} - \langle \phi_i | \phi_j \rangle), \quad (10)$$

where \mathcal{E} appears due to normalization constraint of the trial many-body function (8), and μ_{ij} – due to orthonormalization of all one-particle functions. To find the minimum of this functional we put to zero all first derivatives of this functional with respect to every $C_{(n_1, n_2, n_3, \dots, n_M)}^*$ and ϕ_i^* appearing in the expansion Eq.(8):

$$\frac{\partial \mathcal{L}[\{C_{\vec{n}}\}, \{\phi_i\}]}{\partial C_{\vec{n}}^*} = 0 = \sum_{\vec{n}'} C_{\vec{n}'} \langle \vec{n} | \hat{H} | \vec{n}' \rangle - \mathcal{E} C_{\vec{n}}, \quad \forall \vec{n} \quad (11a)$$

$$\frac{\delta \mathcal{L}[\{C_{\vec{n}}\}, \{\phi_i\}]}{\delta \phi_i^*} = 0 = \frac{\delta \langle \Psi | \hat{H} | \Psi \rangle}{\delta \phi_i^*} - \mu_{i1} |\phi_1\rangle - \mu_{i2} |\phi_2\rangle \dots - \mu_{iM} |\phi_M\rangle, \quad i = 1, \dots, M. \quad (11b)$$

Here we used partial derivatives and functional derivatives to separate the variations with respect to the expansion coefficients and the one-particle functions. Such a separation is permitted because μ_{ij} and ϕ_i do not depend explicitly on $C_{\vec{n}}$. Eq.(11a) defines the expansion coefficients when the set of the one-particle functions is given, while Eq.(11b) finds the best, i.e., energetically most favorable one-particle functions when the set of the expansion coefficients $C_{\vec{n}}$ is known.

We can use the following strategy to solve the two-fold variational problem Eqs.(11a) and (11b) *self-consistently*. Starting from some guess for the orbitals $\{\phi_i\}$ we construct the initial many-body basis set. Then we use these initial fixed-orbital many-body basis functions to build up the secular Hamiltonian matrix. As we shall see in the subsequent Sec.II B 1, the

first part of the variational principle Eq.(11a), i.e., the problem of finding the unknown coefficients $C_{(n_1, n_2, n_3, \dots, n_M)}$ can be reduced to the diagonalization of the secular Hamiltonian matrix. The expansion coefficients obtained as the components of the respective eigenvector are utilized in the second part of the variational procedure Eq.(11b) which provides as its output a new approximation to the one-particle functions $\{\phi_i\}$, see for details Sec.II B 2. This iterative scheme is repeated until convergence is achieved. We call the obtained optimal set of the one-particle functions and respective expansion coefficients the self-consistent solution.

Since in this approach the many-body bosonic wave-function is presented as a sum of all possible configurations (symmetrized Hartree products) resulting as permutations of N bosons over M orbitals, we name this general variational method Multi-Configurational Hartree for Bosons or MCHB(M). Here M specifies explicitly the number of one-particle functions involved.

1. Variations with respect to the expansion coefficients $\{C_{\vec{n}}\}$ and general rules for evaluating matrix elements with permanents

The quantities $\langle \vec{n} | \hat{H} | \vec{n}' \rangle$ appearing in Eq.(11a) are the matrix elements of a matrix Hamiltonian \mathcal{H} . This system of equations can be written in matrix notations as

$$\mathcal{H}\mathbf{C} = \mathcal{E}\mathbf{C}, \tag{12}$$

where \mathbf{C} is a column vector of the expansion coefficients $C_{\vec{n}}$. As usual, the problem of finding the expansion coefficients $\{C_{\vec{n}}\}$ for a given set of one-particle functions $\{\phi_i\}$ boils down to an eigenvalue problem. This opens the possibility to attack not only the ground, but also excited states.

The main issue now is to evaluate the matrix elements $\langle \vec{n} | \hat{H} | \vec{n}' \rangle$ with permanents. As introduced in Eq.(4), the Hamiltonian is made of an one-particle operator \hat{h} and of a two-body inter-particle interaction operator \hat{W} . It is useful to treat these one-body $\langle \vec{n} | \hat{h} | \vec{n}' \rangle$ and two-body $\langle \vec{n} | \hat{W} | \vec{n}' \rangle$ interaction terms individually.

In the following we report the general rules to evaluate the matrix elements of one-body and two-body operators. For simplicity these operators are denoted \hat{h} and \hat{W} although they need not be the constituents of the Hamiltonian. Let us distinguish between six generic

types of permanents:

$$\begin{aligned}
|P_0\rangle &= |n_1, n_2, \dots, n_i, \dots, n_j, \dots, n_M\rangle \equiv |; n_i; n_j; \rangle \\
|P_1\rangle &= |n_1, n_2, \dots, n_i + 1, \dots, n_j - 1, \dots, n_M\rangle \equiv |; n_i + 1; n_j - 1; \rangle \\
|P_2\rangle &= |n_1, n_2, \dots, n_i + 2, \dots, n_j - 2, \dots, n_M\rangle \equiv |; n_i + 2; n_j - 2; \rangle \\
|P_3\rangle &= |n_1, n_2, \dots, n_i + 2, \dots, n_j - 1, \dots, n_k - 1, \dots, n_M\rangle \equiv |; n_i + 2; n_j - 1; n_k - 1; \rangle \\
|P_4\rangle &= |n_1, n_2, \dots, n_i + 1, \dots, n_j + 1, \dots, n_k - 2, \dots, n_M\rangle \equiv |; n_i + 1; n_j + 1; n_k - 2; \rangle \\
|P_5\rangle &= |n_1, n_2, \dots, n_i + 1, \dots, n_j + 1, \dots, n_k - 1, \dots, n_l - 1, \dots, n_M\rangle \\
&\equiv |; n_i + 1; n_j + 1; n_k - 1; n_l - 1; \rangle.
\end{aligned} \tag{13}$$

The permanent $|P_1\rangle$ can be obtained from $|P_0\rangle$ by excitation of a single boson from ϕ_j to ϕ_i . The other four permanents, $|P_2\rangle$ to $|P_5\rangle$, describe two-boson excitations of $|P_0\rangle$. To shorten the notations we show only the occupation numbers of the involved orbitals. For instance, the configuration $(; n_i - 1; n_j + 1;)$ differs from $\vec{n} \equiv (; n_i; n_j;)$ by an excitation of a single boson from ϕ_i to ϕ_j . We stress that only if two permanents differ by the excitation of at most two bosons, the Hamiltonian matrix element evaluated with these permanents is non-zero. All other permanents give vanishing matrix elements.

The matrix elements of an one-body operator \hat{h} are non-zero if the two permanents are either equal (diagonal contributions) or differ by an excitation of a single boson:

$$\begin{aligned}
\langle P_0 | \hat{h} | P_0 \rangle &= \langle ; n_i; n_j; | \sum_{\alpha, \beta=1}^M h_{\alpha\beta} b_\alpha^\dagger b_\beta | ; n_i; n_j; \rangle = \sum_{\alpha=1}^M h_{\alpha\alpha} n_\alpha, \\
\langle P_1 | \hat{h} | P_0 \rangle &= \langle ; n_i + 1; n_j - 1; | \hat{h} | ; n_i; n_j; \rangle = h_{ij} \sqrt{n_i + 1} \sqrt{n_j}.
\end{aligned} \tag{14}$$

The diagonal matrix elements of a two-body operator \hat{W} are:

$$\begin{aligned}
\langle P_0 | \hat{W} | P_0 \rangle &= \langle ; n_i; n_j; | \sum_{\alpha, \beta, \gamma, \delta} \frac{1}{2} W_{\alpha\beta\gamma\delta} b_\alpha^\dagger b_\beta^\dagger b_\gamma b_\delta | ; n_i; n_j; \rangle \\
&= \frac{1}{2} \sum_{\alpha}^M n_\alpha (n_\alpha - 1) W_{\alpha\alpha\alpha\alpha} + \frac{1}{2} \sum_{\beta \neq \alpha=1}^M n_\alpha n_\beta (W_{\alpha\beta\alpha\beta} + W_{\alpha\beta\beta\alpha}).
\end{aligned} \tag{15}$$

The matrix elements of a two-body operator \hat{W} evaluated with permanents which differ by the excitation of one boson read:

$$\begin{aligned}
\langle P_1 | \hat{W} | P_0 \rangle &= \langle ; n_i + 1; n_j - 1; | \hat{W} | ; n_i; n_j; \rangle \\
&= \frac{1}{2} \sqrt{n_i + 1} \sqrt{n_j} \left[\sum_{\alpha=1, \alpha \neq i, j}^M n_\alpha (W_{i\alpha\alpha j} + W_{i\alpha j\alpha}) + n_i W_{iijj} + (n_j - 1) W_{ijjj} \right].
\end{aligned} \tag{16}$$

The permanents which differ by the excitations of two bosons give the following matrix elements of the two-body operator \hat{W} :

$$\begin{aligned}
\langle P_2 | \hat{W} | P_0 \rangle &= \langle ; n_i + 2; n_j - 2; | \hat{W} | ; n_i; n_j; \rangle \\
&= \frac{1}{2} \sqrt{(n_j - 1)n_j} \sqrt{(n_i + 2)(n_i + 1)} W_{iijj}, \\
\langle P_3 | \hat{W} | P_0 \rangle &= \langle ; n_i + 2; n_j - 1; n_k - 1; | \hat{W} | ; n_i; n_j; \rangle \\
&= \sqrt{(n_i + 2)(n_i + 1)} \sqrt{n_j n_k} W_{iijk}, \\
\langle P_4 | \hat{W} | P_0 \rangle &= \langle ; n_i + 1; n_j + 1; n_k - 2; | \hat{W} | ; n_i; n_j; \rangle \\
&= \sqrt{n_k(n_k - 1)} \sqrt{(n_i + 1)(n_j + 1)} W_{ijkk}, \\
\langle P_5 | \hat{W} | P_0 \rangle &= \langle ; n_i + 1; n_j + 1; n_k - 1; n_l - 1; | \hat{W} | ; n_i; n_j; \rangle \\
&= \sqrt{(n_i + 1)(n_j + 1)} \sqrt{n_k n_l} (W_{ijkl} + W_{jikl}). \tag{17}
\end{aligned}$$

In summary, we have demonstrated that for any set of orthogonal one-particle functions $\{\phi_i\}$ used to construct the many-body basis functions, i.e., the permanents, the variational problem of finding the unknown coefficients $C_{(n_1, n_2, n_3, \dots, n_M)}$ is reduced to the diagonalization of the Hamiltonian secular matrix. To construct the secular Hamiltonian matrix we have developed rules for evaluating the matrix elements of the \hat{h} and \hat{W} operators. Due to the generality of the consideration, the developed rules are, of course, applicable for any one- and two-body operators.

2. Variations with respect to the orbitals $\{\phi_i\}$

The functional differentiation of the energy functional Eq.(10) with respect to the one-particle functions ϕ_i^* results in a system of M coupled integro-differential equations

$$\frac{\delta \langle \Psi | \hat{H} | \Psi \rangle}{\delta \phi_i^*} = \mu_{i1} |\phi_1\rangle + \mu_{i2} |\phi_2\rangle \cdots + \mu_{iM} |\phi_M\rangle, \quad i = 1, \dots, M. \tag{18}$$

By solving these equations for given fixed values of the coefficients $C_{\vec{n}}$ one obtains the respective set of the one-particle functions $\{\phi_i\}$.

The main purpose of this section is to express these equations in an explicit form. To fulfil this goal, we first re-write the expectation value of the Hamiltonian, Eq.(9), in a form where all the terms depending on orbitals are explicitly visualized and then apply functional differentiations.

The expectation value of the Hamiltonian can be rewritten in the following form:

$$\langle \Psi | \hat{H} | \Psi \rangle = \sum_{i,j}^M \rho_{ij} h_{ij} + \frac{1}{2} \sum_{i,j,k,l}^M \rho_{ijkl} W_{ijkl}. \quad (19)$$

Here, $\rho_{ij} = \langle \Psi | b_i^\dagger b_j | \Psi \rangle$ are the elements of the reduced one-body density matrix:

$$\begin{aligned} \rho(\vec{r}_1 | \vec{r}'_1) &= N \int \Psi^*(\vec{r}'_1, \vec{r}_2, \dots, \vec{r}_N) \Psi(\vec{r}_1, \vec{r}_2, \dots, \vec{r}_N) d\vec{r}_2 d\vec{r}_3 \dots d\vec{r}_N \\ &= \sum_{i,j}^M \rho_{ij} \phi_i^*(\vec{r}'_1) \phi_j(\vec{r}_1), \end{aligned} \quad (20)$$

and $\rho_{ijkl} = \langle \Psi | b_i^\dagger b_j^\dagger b_k b_l | \Psi \rangle$ are the elements of the two-body density matrix:

$$\begin{aligned} \rho(\vec{r}_1, \vec{r}_2 | \vec{r}'_1, \vec{r}'_2) &= N(N-1) \int \Psi^*(\vec{r}'_1, \vec{r}'_2, \vec{r}_3, \dots, \vec{r}_N) \Psi(\vec{r}_1, \vec{r}_2, \vec{r}_3, \dots, \vec{r}_N) d\vec{r}_3 \dots d\vec{r}_N \\ &= \sum_{i,j,k,l}^M \rho_{ijkl} \phi_i^*(\vec{r}'_1) \phi_j^*(\vec{r}'_2) \phi_k(\vec{r}_1) \phi_l(\vec{r}_2). \end{aligned} \quad (21)$$

The matrix elements of the reduced one- and two-particle densities can be easily obtained:

$$\rho_{ii} = \sum_{\vec{n}} C_{\vec{n}}^* C_{\vec{n}} n_i \equiv \langle \hat{n}_i \rangle,$$

$$\rho_{ij} = \sum_{\vec{n}} C_{\vec{n}}^* C_{(n_i-1; n_j+1)} \sqrt{n_i(n_j+1)}, \quad (22)$$

$$\rho_{iiii} = \sum_{\vec{n}} C_{\vec{n}}^* C_{\vec{n}} (n_i^2 - n_i) \equiv \langle \hat{n}_i^2 \rangle - \langle \hat{n}_i \rangle,$$

$$\rho_{ijij} = \sum_{\vec{n}} C_{\vec{n}}^* C_{\vec{n}} n_i n_j \equiv \langle \hat{n}_i \hat{n}_j \rangle. \quad (23)$$

Here we present only the diagonal matrix elements of the two-particle density; the off-diagonal ones are collected in Appendix A.

Inspecting Eqs.(22) and (23) we see that the matrix elements of the one- and two-particle densities depend only on the expansion coefficients $C_{\vec{n}}$ and do not depend on the one-particle orbitals $\{\phi_i\}$ explicitly. In other words, only the one- and two-body integrals h_{ij} , W_{ijkl} appearing in Eq.(19) have a functional dependence on the one-particle functions ϕ_i^* . Hence,

the functional differentiation has to be applied only to the integrals h_{ij} , W_{ijkl} which we treat individually according to the general rules of functional differentiation:

$$\frac{\delta h_{ij}}{\delta \phi_i^*} = \frac{\delta \langle \phi_i^* | \hat{h} | \phi_j \rangle}{\delta \phi_i^*} = \hat{h} | \phi_j \rangle, \quad (24)$$

$$\frac{\delta W_{ijkl}}{\delta \phi_i^*} = \frac{\delta \langle \phi_i^* \phi_j^* | \hat{W} | \phi_k \phi_l \rangle}{\delta \phi_i^*} = \hat{W}_{jl} | \phi_k \rangle, \quad i \neq j, \quad (25)$$

where we introduce the notation

$$\hat{W}_{jl} = \int \phi_j^*(\vec{r}') W(\vec{r} - \vec{r}') \phi_l(\vec{r}') d\vec{r}' \quad (26)$$

for the *local* operators \hat{W}_{jl} .

Using Eqs.(24,25,26) the variation of the expectation value of the Hamiltonian, Eq.(19), with respect to the ϕ_i^* takes on the following very compact and appealing form

$$\frac{\delta \langle \Psi | \hat{H} | \Psi \rangle}{\delta \phi_i^*} = \sum_{j=1}^M [\rho_{ij} \hat{h} + \sum_{k,l=1}^M \rho_{ikjl} \hat{W}_{kl}] | \phi_j \rangle. \quad (27)$$

Finally, the functional differentiations of the Lagrange energy functional Eq.(10) with respect to the one-particle functions result in a system of M coupled integro-differential equations:

$$\sum_{j=1}^M [\rho_{ij} \hat{h} + \sum_{k,l=1}^M \rho_{ikjl} \hat{W}_{kl}] | \phi_j \rangle = \sum_{j=1}^M \mu_{ij} | \phi_j \rangle, \quad i = 1, \dots, M. \quad (28)$$

The main result of the present section is as follows. For any given set of the expansion coefficients $C_{\vec{n}}$, the best, i.e., energetically most favorable set of one-particle functions $\{\phi_i\}$ used to construct the many-body basis functions (permanents) is determined by solving Eq.(28).

C. Properties of the MCHB(M) equations

In the formulation of MCHB(M) we assumed that the expansion Eq.(8) spans *all* possible configurations of N bosons over M one-particle functions. However, the derived equations for the optimal expansion coefficients (12) and orbitals (28) are general and remain valid even in the case when the expansion Eq.(8) is incomplete and comprises any limited subset of configurations. Let us first consider the simplest limiting case, where the expansion Eq.(8)

contains only a single permanent in which all N bosons reside in one and the same orbital ϕ_1 :

$$|\Psi\rangle = C_{(n_1)}|n_1\rangle. \quad (29a)$$

Of course, $n_1 = N$ due to the conservation of the total number of particles and $C_{(n_1)} \equiv 1$ due to the normalization of $|\Psi\rangle$. Then, the expectation value of the Hamiltonian Eq.(19) takes on the simple form

$$\langle\Psi|\hat{H}|\Psi\rangle = \rho_{11}h_{11} + \frac{1}{2}\rho_{1111}W_{1111} \quad (29b)$$

and Eq.(25) now reads

$$\left\{\rho_{11}\hat{h} + \rho_{1111}\hat{W}_{11}\right\}|\phi_1\rangle = \mu_{11}|\phi_1\rangle. \quad (29c)$$

The respective non-zero elements of the reduced one- and two-body density matrices Eqs.(22,23) become trivial

$$\rho_{11} = \langle\hat{n}_1\rangle \equiv N,$$

$$\rho_{1111} = \langle\hat{n}_1^2 - \hat{n}_1\rangle \equiv N(N - 1). \quad (29d)$$

Obviously, for contact inter-particle interaction $W(\vec{r} - \vec{r}') = \lambda_0\delta(\vec{r} - \vec{r}')$ and putting $\phi_1 \equiv \varphi$ we easily reproduce the famous GP mean-field energy functional

$$E_{GP} = \langle\Psi|\hat{H}|\Psi\rangle = N\left[h_{11} + \frac{N-1}{2}\lambda_0 \int \varphi(\vec{r})^4 d\vec{r}\right] \quad (29e)$$

and the GP equation for the optimal orbital

$$\left\{-\frac{\hbar^2}{2m}\nabla_{\vec{r}}^2 + V(\vec{r}) + \lambda_0(N-1)|\varphi(\vec{r})|^2\right\}|\varphi\rangle = \mu_{GP}|\varphi\rangle, \quad (29f)$$

where $\mu_{GP} \equiv \mu_{11}/N$.

Next, let us demonstrate that in the more general one-configurational case, when the permanent is given by Eq.(2), the many-body MCHB(M) theory boils down to the multi-orbital BMF theory [20, 21, 22]. In this case the only permanent contributing to the expansion Eq.(8) with $C_{(n_1, n_2, \dots, n_M)} = 1$ represents a configuration with n_1 bosons residing in ϕ_1 , n_2 in ϕ_2 , ... n_M in ϕ_M . Let us first rewrite the general expression for the total energy Eq.(19) in a form where the diagonal E_{MF} and off-diagonal E_{MB} contributions are separated:

$$\langle\Psi|\hat{H}|\Psi\rangle = E_{MF} + E_{MB} \quad (30a)$$

where

$$E_{MF} = \sum_{i=1}^M [\rho_{ii} h_{ii} + \frac{1}{2} \rho_{iiii} W_{iiii} + \frac{1}{2} \sum_{j=1, j \neq i}^M (\rho_{ijij} W_{ijij} + \rho_{ijji} W_{ijji})], \quad (30b)$$

and

$$E_{MB} = \sum_{i,j=1, i \neq j}^M (\rho_{ij} h_{ij} + \frac{1}{2} \sum_{\{i,j,k,l\}} \rho_{ijkl} W_{ijkl}), \quad (30c)$$

where $\{i, j, k, l\}$ runs over all possibilities not included in the respective E_{MF} part. Since only one configuration forms the many-body expansion, only the diagonal matrix elements of the reduced one- and two-body density matrices given in Eqs.(22,23) have non-zero values:

$$\rho_{ii} \equiv \langle \hat{n}_i \rangle = n_i,$$

$$\rho_{iiii} \equiv \langle \hat{n}_i^2 - \hat{n}_i \rangle = n_i^2 - n_i,$$

$$\rho_{ijij} = \rho_{ijji} \equiv \langle \hat{n}_i \hat{n}_j \rangle = n_i n_j. \quad (30d)$$

Consequently, $E_{MB} = 0$ and only the E_{MF} part of the total energy survives and boils down to

$$\langle \Psi | \hat{H} | \Psi \rangle = E_{MF} = \sum_{i=1}^M n_i [h_{ii} + \frac{n_i - 1}{2} W_{iiii} + \sum_{j=1, j \neq i}^M n_j (W_{ijij} + W_{ijji})]. \quad (30e)$$

Analogously, Eq.(28) determining the optimal orbitals now reads:

$$[n_i \hat{h} + n_i(n_i - 1) \hat{W}_{ii} + \sum_{j=1, j \neq i}^M n_i n_j \hat{W}_{jj}] |\phi_i\rangle + \sum_{j=1, j \neq i}^M n_i n_j \hat{W}_{ji} |\phi_j\rangle = \sum_{j=1}^M \mu_{ij} |\phi_j\rangle, \quad i = 1, \dots, M. \quad (31)$$

These equations coincide with the multi-orbital mean-field equations, formulated and applied in Refs.[20, 21, 22, 23, 24].

We conclude that in the limiting cases where only one permanent forms the many-body expansion Eq.(8), the many-body MCHB(M) theory boils down to the respective mean-fields. On the other hand, if only one configuration in the many-body expansion is dominant, then the multi-orbital mean-field predictions are very close to the many-body ones. Such a situation can be realized in real physical systems, for example in deep multi-well traps.

When the expansion Eq.(8) spans *all* possible configurations of N bosons over M one-particle functions, the MCHB(M) equations possess some interesting and useful properties. Suppose we solve this system of equations and find the optimal orbitals $\{\phi_i\}$ and corresponding expansion coefficients $\{C_{(n_1, n_2, n_3, \dots, n_M)}\}$. By applying an unitary transformation on the

ϕ_i we can construct a new set of the one-particle functions and find the corresponding new set of the expansion coefficients $\{\tilde{C}_{(n_1, n_2, n_3, \dots, n_M)}\}$. This unitary transformation does not change (up to a phase factor) the many-body wave-function Eq.(8). Consequently, the total energy $\langle \Psi | \hat{H} | \Psi \rangle$ of the system is invariant with respect to any unitary transformation of the one-particle functions. Moreover, we can demonstrate that this is also valid at any iteration during the described procedure leading to the self-consistent solution of the MCHB(M) equations. The considered invariance of the equations is explained by the fact that the expansion Eq.(8) spans *all* possible configurations, i.e., it is *complete* within the provided subspace of one-particle functions. Clearly, for an incomplete expansion this invariance is, in general, lost. For instance, it was shown that the multi-orbital mean-field equations [20, 21, 22], which, as discussed above, can be considered as one-particle MCHB(M) equations, indeed are in general not invariant with respect to unitary transformations of the orbitals $\{\phi_i\}$.

Having established the equivalence of the MCHB(M) solutions with respect to unitary transformations, it is natural to find out which set of orbitals can provide additional physical insight. Since the energy is invariant, we consider the reduced one- and two-particle density matrices. Having at hand a reduced one-particle density matrix one can diagonalize it:

$$\rho(\vec{r}|\vec{r}') = \sum_i^M \rho_i \phi_i^{*NO}(\vec{r}') \phi_i^{NO}(\vec{r}). \quad (32)$$

The eigenvectors ϕ_i^{NO} are referred to as *natural orbitals* and the eigenvalues ρ_i of this matrix are the respective *occupation numbers*. The natural occupation numbers ρ_i can be considered as the average numbers of bosons residing in ϕ_i^{NO} . The natural orbital analysis of the many-body solution is often used to characterize the system. The system is condensed [32] when only a single natural orbital has a macroscopic occupation. If several natural orbitals have macroscopic occupation numbers then the system is called *fragmented* [33]. Of course, the natural orbital analysis can be applied to any state, also to excited states. Comparing the natural orbitals and occupation numbers of the ground and excited states one can learn on the nature of the excited state.

Let us examine the properties of the natural orbitals in the MCHB(M) theory. On the one hand, we know that each eigenvector of the one-body density matrix $\rho(\vec{r}|\vec{r}')$ can be expressed as a linear combination of the MCHB(M) orbitals. On the other hand, we have seen that due to the completeness of the many-body expansion, the MCHB(M) solution is invariant

with respect to any unitary transformation applied. We conclude that the natural orbitals themselves constitute a MCHB(M) solution as well. This finding gives us the freedom to characterize the MCHB(M) one-particle functions by natural orbitals. We shall do so in the following, unless explicitly mentioned.

Using the multi-configurational expansion Eq.(3) as an ansatz for the true many-body wave function of a trapped bosonic system and applying the variational principle we derived general equations which allow one to find the best many-body basis functions and the corresponding expansion coefficients self-consistently. We have shown that these equations are also applicable in any desired active sub-space, including the limiting case of one-particle. In the latter case the derived equations boil down to the one-orbital Gross-Pitaevskii and multi-orbital mean-fields equations. At this point it is very important to stress that all derived equations and conclusions are general, i.e., they are valid for any geometry of the external trap potential, for any physical shape of the inter-particle interaction and in any dimension.

III. ILLUSTRATIVE NUMERICAL EXAMPLES AND APPLICATIONS

A. Preliminaries and implementation of MCHB(2)

In the present section we implement the developed MCHB(M) formalism for systems of cold bosonic atoms. We consider the simplest case of M=2, i.e., MCHB(2) theory and apply it to the ground and excited states of the bosonic systems trapped in symmetric and asymmetric one- and two- dimensional double-well potentials. While the ground state of the one-dimensional bosonic gas trapped in symmetric double-well potentials has been intensively studied in the literature see Refs.[30, 31, 34, 35] and references therein, the many-body properties of bosonic systems at higher dimensions in symmetric and especially asymmetric double-well traps [36] are open theoretical questions.

The configurational space of the MCHB(2) theory constitutes all symmetrized permutations of N bosons over two orbitals ϕ_1 and ϕ_2 . The trial many-body function Eq.(3) in this case is spanned by N+1 configurations:

$$|\Psi\rangle = \sum_{n_1=0}^N C_{(n_1, n_2)} |n_1, n_2\rangle \quad (33)$$

The condition $n_1 + n_2 = N$ implies that only one occupation number n_1 can be used to enumerate the configurations.

The configurational space of MCHB(2) theory also implies that the non-zero Hamiltonian matrix elements can be only between the three generic permanents

$$|P_0\rangle = |n_1, n_2\rangle, |P_1\rangle = |n_1 + 1, n_2 - 1\rangle, |P_2\rangle = |n_1 + 2, n_2 - 2\rangle. \quad (34)$$

Using these permanents and the general rules for evaluating one-body and two-body matrix elements, Eqs.(14,15,16,17), the expectation value of the Hamiltonian (19) becomes

$$\begin{aligned} \langle \Psi | \hat{H} | \Psi \rangle &= \langle \hat{n}_1 \rangle h_{11} + \langle \hat{n}_2 \rangle h_{22} \\ &+ \frac{\langle \hat{n}_1^2 \rangle - \langle \hat{n}_1 \rangle^2}{2} W_{1111} + \frac{\langle \hat{n}_2^2 \rangle - \langle \hat{n}_2 \rangle^2}{2} W_{2222} + \langle \hat{n}_1 \hat{n}_2 \rangle (W_{1212} + W_{1221}) \\ &+ \rho_{12} h_{12} + \rho_{21} h_{21} + \rho_{2111} W_{2111} + \rho_{1112} W_{1112} \\ &+ \rho_{2221} W_{2221} + \rho_{1222} W_{1222} + \frac{\rho_{2211}}{2} W_{2211} + \frac{\rho_{1122}}{2} W_{1122}. \end{aligned} \quad (35)$$

The coupled system of integro-differential equations (28) needed for determination of the optimal one-particle functions reads:

$$\begin{aligned} &\left\{ \langle \hat{n}_1 \rangle \hat{h} + (\langle \hat{n}_1^2 \rangle - \langle \hat{n}_1 \rangle^2) \hat{W}_{11} + \langle \hat{n}_1 \hat{n}_2 \rangle \hat{W}_{22} + \rho_{2111} \hat{W}_{21} + \rho_{1112} \hat{W}_{12} \right\} |\phi_1\rangle + \\ &\quad \left\{ \langle \hat{n}_1 \hat{n}_2 \rangle \hat{W}_{21} + \rho_{1112} \hat{W}_{11} + \rho_{12} \hat{h} + \rho_{1222} \hat{W}_{22} + \rho_{1122} \hat{W}_{12} \right\} |\phi_2\rangle = \mu_{11} |\phi_1\rangle + \mu_{12} |\phi_2\rangle \\ &\left\{ \langle \hat{n}_2 \rangle \hat{h} + (\langle \hat{n}_2^2 \rangle - \langle \hat{n}_2 \rangle^2) \hat{W}_{22} + \langle \hat{n}_1 \hat{n}_2 \rangle \hat{W}_{11} + \rho_{2221} \hat{W}_{21} + \rho_{1222} \hat{W}_{12} \right\} |\phi_2\rangle + \\ &\quad \left\{ \langle \hat{n}_1 \hat{n}_2 \rangle \hat{W}_{12} + \rho_{2221} \hat{W}_{22} + \rho_{21} \hat{h} + \rho_{2111} \hat{W}_{11} + \rho_{2211} \hat{W}_{21} \right\} |\phi_1\rangle = \mu_{21} |\phi_1\rangle + \mu_{22} |\phi_2\rangle. \end{aligned} \quad (36)$$

As an illustrative example we consider N identical spinless bosons, interacting via contact potential $W(\vec{r} - \vec{r}') = \lambda_0 \delta(\vec{r} - \vec{r}')$, where λ_0 is proportional to the s -wave scattering length. In this case the two-body integrals, see Eq.(6), appearing in Eq.(35) simplify to

$$W_{ijkl} = \lambda_0 \int \phi_i^*(\vec{r}) \phi_j^*(\vec{r}') \phi_k(\vec{r}) \phi_l(\vec{r}') d\vec{r},$$

and instead of the local integral operators appearing in Eq.(36) we obtain the functions

$$\hat{W}_{ij} = \lambda_0 \phi_i^*(\vec{r}) \phi_j(\vec{r}).$$

This considerably simplifies the implementation of the MCHB theory as the system of integro-differential equations (36) boils down to a system of *non-linear* coupled differential equations. Furthermore, in this paper we work in $\frac{\hbar^2}{L^2 m} = 1$ units, where m is the mass of boson and L is the length scale.

We recall that for MCHB(2) theory the number of particles, the inter-particle interaction strength λ_0 and the external trap potential have to be specified. The expansion coefficients $\{C_{(n_1, n_2)}\}$ and orbitals ϕ_1 and ϕ_2 are treated as variational parameters. The optimal values of these parameters are determined *self-consistently* by diagonalizing the secular Hamiltonian matrix to find the expansion coefficients, Eq.(12), and by solving the coupled system of non-eigenvalue non-linear differential equations Eq.(36) to get the one-particle functions.

The self-consistent procedure of finding the optimal one-particle functions and corresponding expansion coefficients can be implemented as follows. We start from some initial guess for the one-particle functions ϕ_1, ϕ_2 obtained, say, as the two eigenfunctions lowest in energy of the *bare* Hamiltonian

$$\hat{h}\phi_i = \left[-\frac{1}{2}\nabla_{\vec{r}}^2 + V(\vec{r}) \right] \phi_i = \epsilon_i\phi_i, \quad (37)$$

where $i = 1, 2$ and $V(\vec{r})$ is the corresponding trap potential. These one-particle functions are used to construct the permanents in the expansion Eq.(33) and to evaluate the Hamiltonian matrix elements. By diagonalizing this matrix, we solve the corresponding secular equation Eq.(12) and get $N+1$ orthonormal eigenfunctions and the corresponding eigenvalues. The lowest-energy solution corresponds to the ground state of the problem, while other solutions may be used to attack excited states. The eigenvector of interest contains the set of expansion coefficients $\{C_{(n_1, n_2)}\}$. To implement the second part of the variational principle, we use these expansion coefficients to evaluate the elements of the reduced one- and two-body densities given in Eqs.(22,23) and in Appendix A, required by the coupled system (36) of the MCHB(2) equations. By solving this system of equations we find a new set of the one-particle functions ϕ_1, ϕ_2 . This self-consistent scheme is iterated until convergence is achieved.

One goal here is to demonstrate that when the bosonic system is treated at the many-body level and the many-body basis set is incomplete, then the choice of one-particle functions used to construct this many-body basis set has a great impact on the results and predictions obtained. To realize this in practice we consider two sets of one-particle functions and compare the many-body predictions obtained within each set. As the first set we use the lowest-energy eigenfunctions of the bare Hamiltonian Eq.(37). We stress that such a fixed choice of the one-particle functions is often used [26, 27, 28] in many-body treatments on bosonic systems. The MCHB(2) solution is the second set of orbitals which is, of course, the best possible choice because these orbitals have been obtained in the framework of the full

variational principle. From now on we use BH and MCHB superscripts to distinguish the results obtained within bare Hamiltonian and MCHB(2) one-particle function sets, respectively. For example, we denote the corresponding one-particle functions as ϕ_1^{BH}, ϕ_2^{BH} and $\phi_1^{MCHB}, \phi_2^{MCHB}$. In our iterative MCHB(2) scheme we use ϕ_1^{BH}, ϕ_2^{BH} as the initial guess. Therefore, by comparing the results obtained at the first and last iterations we immediately observe the impact of self-consistency.

Let us now elaborate on the choice of trapping potentials. In our work we have chosen the following form of symmetric and asymmetric double-well potentials. Let us imagine two separate trap potentials, for simplicity in 1D, described by $V_1(x)$ and $V_2(x)$. We construct a "superposition" of these traps in such a way that, on the one hand, the profiles of each potential well in the resulting double-well potential would be as much as possible close to the original potentials. On the other hand, it is also desirable that the inter-trap separation, degree of asymmetry and barrier height can be easily manipulated. What is also important is that this double-well potential would have a simple (differentiable) analytic form and permit 2D and 3D generalizations. Let us diagonalize the matrix

$$\begin{pmatrix} V_1(x+x_0) + B & C \\ C & V_2(x-x_0) \end{pmatrix}. \quad (38)$$

The lowest eigenvalue of this matrix is a function which fulfils almost all the above mentioned requirements. The original traps are connected to each other and the parameter C is responsible for the smoothness of this connection. The minima of the wells are located approximatively at $\pm x_0$ and the $V_1(x)$ trap is biased by B with respect to the $V_2(x)$ one. However, to gain an additional control on the barrier height we add a smooth barrier function centered at the origin:

$$V_b(A, D) = \frac{A}{\sqrt{2\pi}D} \exp \frac{-x^2}{2D^2}, \quad (39)$$

where D defines the width of this additional barrier function and A can be used to vary its height. The resulting trap potential takes on an analytic form:

$$V(x) = \frac{1}{2} [V_1(x+x_0) + B - \sqrt{4C^2 + (V_1(x+x_0) + B - V_2(x-x_0))^2} + V_2(x-x_0)] + V_b(A, D).$$

We recall that in this paper we work in $\frac{\hbar^2}{L^2 m} = 1$ units, where m is the mass of boson and L is the length scale.

B. Ground state in 1D symmetric double-well trap

Let us first apply MCHB(2) theory to study the ground state of repulsive bosons trapped in a symmetric double-well potential. This is a popular problem, widely discussed in the literature, see Refs.[30, 31, 34, 35] and references therein. We consider a system of $N=1000$ bosons which is of the order of the particle number taken in recent experiments [9]. This system is trapped in the symmetric double-well potential:

$$V_{symm}(x) = 0.5x^2 - \frac{1}{2}\sqrt{25 + 64x^2} + 8.19531 + V_b(A = 4, D = 0.75). \quad (40)$$

This potential plotted in the left panel of Fig.1 by a thick solid(black) line is obtained by diagonalizing Eq.(38) with $V_1(x) = 0.5(x + 4.0)^2$, $V_2(x) = 0.5(x - 4.0)^2$, $C = 2.5$, $B = 0.0$ and by adding a barrier function $V_b(A = 4, D = 0.75)$ (see Eq.(39)). A constant shift has been applied to put the minimum of the potential energy to zero.

In the right panel of Fig.1 we plot the ground state energies per particle of this system as a function of the inter-particle interaction strength λ_0 . The many-body results obtained within fixed bare Hamiltonian (BH) one-particle functions are plotted by a solid (black) line with open circles. The solid (red) line with filled circles represents the energies per particle obtained self-consistently within the framework of the MCHB(2) theory. Both curves coincide only at the limit of non-interacting particles, the optimal one-particle functions in this case are the bare Hamiltonian functions. Increasing λ_0 , the MCHB(2) energy curve gradually (exponentially) deviates from the fixed-orbital one. To illustrate this we plot in the inset the difference between these energies per particle $\Delta = E^{BH} - E^{MCHB}$ as a function of λ_0 (notice the logarithmic scale on both axes). It is clearly seen that the many-body treatment with fixed one-particle functions provides an adequate description only up to $\lambda_0 \sim 10^{-3}$. For stronger inter-particle interactions the self-consistency becomes more and more relevant, and leads to lower energies. We conclude that the choice of the one particle functions in truncated CI expansions is very crucial for the appropriate description of the energetics of interacting bosonic systems.

Next, we construct the reduced one-particle density matrix Eq.(22) and find the corresponding natural orbitals and natural occupation numbers Eq.(32). The many-body ansatz used in the MCHB(2) theory implies that there are only two natural orbitals with respective occupations numbers ρ_1 and ρ_2 . The conservation of the total number of particles $\rho_1 + \rho_2 = N$ allows us to consider only one occupation number.

In Fig.2 we plot the occupation number ρ_2 of the second natural orbital as a function of the inter-particle interaction strength λ_0 . The solid (red) line with filled circles and the solid (black) line with open circles represent the self-consistent MCHB(2) and fixed-orbital BH results, respectively. Up to $\lambda_0 \sim 10^{-3}$ both methods predict that the value ρ_2 gradually increases with λ_0 . In other words, according to both many-body treatments fragmentation takes place when λ_0 is increased and at $\lambda_0 \sim 10^{-3}$ approximately 200 particles out of $N = 1000$ are fragmented. However, for $\lambda_0 \geq 10^{-3}$ the predictions obtained within the self-consistent MCHB(2) and the fixed-orbital many-body theory start to deviate from each other and eventually *drastically contradict* each other. The many-body results obtained with fixed bare Hamiltonian functions show that the fragmented fraction ρ_2 increases further with λ_0 until it saturates to some constant value, $\rho_2 \approx 366$. In contrast, the MCHB(2) theory predicts that at some inter-particle interaction strength the ρ_2 fragmented fraction approaches its maximum value and then gradually decreases. Finally, we would like to mention that at much larger values of λ_0 another physical phenomenon starts to take place, fermionization [23, 37], but the region of inter-particle interaction strengths studied here is far below this limit.

Now we elaborate on the physics behind these many-body predictions. The ground state fragmentation phenomenon studied here appears due to the double-well topology of the trap potential and disappears at zero barrier height. With increasing inter-particle interaction the respective chemical potential(s) of the trapped repulsive bosons increase as well and this can be viewed as an effective reduction of the barrier height. The trap potential used in the present study has a barrier of finite height and, hence, from some critical interaction strength on the bosons are energetically above the barrier and do not "see" it. We may thus conclude that the self-consistent MCHB(2) theory predicts a physically relevant behavior of the fragmentation as a function of inter-particle interaction strength in contrast to that predicted by the fixed bare Hamiltonian functions.

Now we investigate the fragmentation phenomenon in the symmetric double-well potential as a function of the barrier height. We ask the question at which barrier height the system of $N = 1000$ bosons at fixed inter-particle interaction strength of $\lambda_0 = 0.01$ becomes, say, 25% fragmented. We consider the same symmetric double-well trap potential as in Eq.(40) and rump the barrier up by varying the parameter A of $V_b(A, D = 0.75)$ (see Eq.(39)). For every A a constant shift is applied to put the minimum of the respective potential energy

to zero, hence $V_{symm}(x)$ at $x = 0$ determines the value of the barrier height. In Fig.3 we plot the occupation number ρ_2 of the second natural orbital as a function of the barrier height. The solid (red) line with filled circles and the solid (black) line with open circles represent the MCHB(2) and fixed-orbital BH results, respectively. In this figure it is clearly seen that 25% fragmentation ratio, i.e., $\rho_2 = 250$ out of $N = 1000$ bosons, is obtained in the framework of fixed-orbital many-body theory at a barrier height $V_{symm}(0) \approx 6.75$, while the self-consistent MCHB(2) gives such a fragmentation ratio when the barrier height is $V_{symm}(0) \approx 10.3$. Again, the BH predictions considerably overestimate the fragmentation. In reality the fragmentation develops slower with increasing barrier height than predicted by the fixed-orbital BH many-body method. This observation is also of a relevance for multi-well systems, including optical lattices. We stress that the difference between predictions of both theories has a non-trivial origin, and one curve can not be obtain from the other by a simple procedure, e.g. shift. To illustrate this, we plot in Fig.3 by dashed (blue) line the difference between corresponding occupation numbers $\Delta = \rho_2^{BH} - \rho_2^{MCHB}$ as a function of the barrier height. In this figure we see that this difference is substantial at any finite barrier heights and becomes less pronounced only in the limit of very large barrier heights.

In these investigations of the ground state of a bosonic system trapped in symmetric double-wells we have seen that the predictions obtained within the framework of the fully self-consistent MCHB(2) and within fixed-orbital many-body theories utilizing the same active space are quantitatively and some times even qualitatively different. By construction, the self-consistent description is more precise than the fixed-orbital one. The fixed-orbital many-body theory can, in principle, reproduce the self-consistent MCHB(2) results if more BH orbitals are included, i.e., if the active space is enlarged, resulting in a substantial increase of the computational effort which can be in practice beyond reach.

C. Ground state in 1D asymmetric double-well trap

Despite considerable progress in the experimental studies on double-well traps [9, 10, 11], a realization of a double-well potential with perfect symmetry is not straightforward. In contrast, bosonic systems trapped in a perfect double-well potential is the most popular theoretical problem addressed in the literature [30, 31, 34, 35], while theoretical studies on bosonic systems in asymmetric traps remain scarce [36]. To elaborate on this very

complicated problem, we address here the ground state of bosonic systems trapped in one-dimensional asymmetric double-well trap potentials. Again, the goal is to demonstrate that self-consistent many-body methods remain of importance.

To construct the asymmetric double-well trap we locate two equal harmonic traps at $\pm x_0$ and displace the left trap upwards with a bias B . Clearly, if the wells are well separated, then the bare eigenfunctions of this trap lowest in energy are predominantly localized either in the left or right wells and keep the shapes of the pure harmonic functions. For a comparatively small bias B , the three eigenstates of the double-well potential lowest in energy are ordered as depicted in the left panel of Fig.4. Such an asymmetric double-well potential can be obtained by diagonalizing Eq.(38) with $V_1(x) = 0.5(x + 4.0)^2$, $V_2(x) = 0.5(x - 4.0)^2$, $C = 2.5$, $B = 0.5$ and by adding a barrier function $V_b(A = 4, D = 0.75)$. A constant shift is also applied to put the global minimum of the potential energy to zero. The analytical function of this potential reads

$$V_{asymm}(x) = 0.5x^2 - \frac{1}{2}\sqrt{25.25 + 8x + 64x^2} + V_b(A = 4, D = 0.75) + 8.4423. \quad (41)$$

We consider $N=1000$ bosons trapped in the asymmetric double-well potential of Eq.(41). Let us see how the ground state of this system develops with increasing inter-particle interaction strength λ_0 . The physical picture of this development, also supported by mean-field studies [21, 23] is as follows. At zero interaction all bosons are localized in the deeper (right) well. The bosons continue to stay localized in this well up to some critical interaction strength λ_0^{cr} . From this λ_0^{cr} on the tunnelling of bosons into the left well becomes possible and bosons start to occupy the left well. In other words, there are two regimes of λ_0 , in the first regime $\lambda_0 < \lambda_0^{cr}$ the ground state properties depend mainly on the geometry of the deeper well, while in the second regime $\lambda_0 > \lambda_0^{cr}$ they depend on the global geometry of the asymmetric double-well potential. These observations are supported by our MCHB(2) calculations presented in the right panel of Fig.4. The MCHB(2) theory gives $\lambda_0^{cr} = 0.00136$ for the transition between the two regimes.

In the right lower panel of Fig.4 one can see that in the first regime ($\lambda_0 = 0.00135 < \lambda_0^{cr}$) both the orbitals and the density are indeed localized in the right well. The natural analysis tells that $\rho_1 = 999.98$ bosons are condensed on the first natural orbital (red) and the fraction of $\rho_2 = 0.02$ bosons is depleted to the second natural orbital (blue). Since both orbitals are localized in the same well, we can say that the origin of the depletion is on-site excitations.

The MCHB natural orbitals and the density for the second regime ($\lambda_0 = 0.01 > \lambda_0^{cr}$) are plotted in the upper right panel of Fig.4 and as it was expected in this case both wells are populated. This ground state is almost 10% fragmented, because $\rho_1 = 906.06$ bosons reside in the first and $\rho_2 = 93.94$ bosons in the second natural orbital.

Let us see whether it is possible at all to obtain qualitatively the same results by using the fixed-orbital many-body method. The bare Hamiltonian functions of the asymmetric double-well potential of Eq.(41) are depicted schematically in the left panel of Fig.4. If the first and second orbitals are used to construct the permanents, then at any non-zero interaction strength the bosons are spread over both wells. Consequently, with such a choice of one-particle functions the first regime can not be described. Instead, one can try to use the first and third eigenfunctions of the bare Hamiltonian to construct the many-body basis set. In this case, however, it is impossible to address the second regime. To overcome this difficulty one can use all three orbitals simultaneously. However the active space, i.e., the number of many-body basis functions used in this case is much larger than the MCHB(2) ones. For $N = 1000$ we would need $\binom{3 + 1000 - 1}{1000} = 501501$ configurations instead of $1001!$ Still, the self-consistency is not used and the quality of these fixed-orbital results has to be investigated.

D. Distributions of the expansion coefficients

So far, to study bosonic systems trapped in the symmetric and asymmetric double-well potentials we have considered and analyzed the MCHB energies and orbitals. We recall that the MCHB solution is given by the optimal sets of one-particle functions and of the respective expansion coefficients obtained self-consistently. In this section we analyze in some detail the MCHB coefficients $\{C_{(n_1, \dots, n_M)}\}$ appearing in the expansion Eq.(8) and exploit the freedom of unitary transformation as put forward in Sec.II C.

Generally, for any orthogonal many-body basis set the square of the expansion coefficient $C_{(n_1, \dots, n_M)}^* C_{(n_1, \dots, n_M)}$ defines the probability to find the many-body solution in the configuration described by the respective many-body basis function $|n_1, n_2, n_3, \dots, n_M\rangle$. In other words, the squares of the expansion coefficients can be considered as a multi-dimensional discrete probability distribution in the discrete sample space spanned by the

many-body basis functions. In the MCHB(2) theory, to count all many-body basis functions $|n_1, n_2\rangle \equiv |n_1, N - n_1\rangle$ one needs only one independent parameter n_1 ($n_2 = N - n_1$). Therefore, the squares of expansion coefficients can be viewed as a probability function $P(n)$ of a discrete distribution defined over the independent parameter $n = 0, 1, 2, \dots, N$:

$$P(n) = C_{(n, N-n)}^* C_{(n, N-n)}. \quad (42)$$

We can use the mean value ν and variance σ^2 as measures of the distribution:

$$\begin{aligned} \nu_{n_1} &= \sum_{n_1=0}^N P(n_1) n_1 = \sum_{n_1=0}^N C_{(n_1, n_2)}^* C_{(n_1, n_2)} n_1 \equiv \langle \hat{n}_1 \rangle, \\ \sigma_{n_1}^2 &= \sum_{n_1=0}^N P(n_1) n_1^2 - \left(\sum_{n_1=0}^N P(n_1) n_1 \right)^2 \equiv \langle \hat{n}_1^2 \rangle - \langle \hat{n}_1 \rangle^2. \end{aligned} \quad (43)$$

Here, we use n_1 as the independent parameter. If the occupation number of the second orbital n_2 is used instead then $\nu_{n_2} = N - \nu_{n_1}$. Interestingly, the $\langle \hat{n}_i \rangle$ and $\langle \hat{n}_i^2 \rangle$ have already appeared in the evaluation of the diagonal elements of the reduced one-particle Eq.(22) and two-particle Eq.(23) density matrices.

As mentioned above in Sec.II C, due to the invariance of the MCHB solution with respect to unitary transformations, there are infinitely many possible choices of the MCHB orbitals which give the same energy. It is also clear that the distribution of the expansion coefficients depends on the particular choice of the one-particle functions used to construct the many-body basis set. Therefore, there are infinitely many possible distributions of the expansion coefficients as well. However, since the mean values and variances of the distributions are different, we use these quantities as the main criteria to compare energetically equivalent distributions. The main aim now is to find the distributions characterized by the *minimal width*.

Let us consider two sets of the MCHB(2) orbitals connected by a unitary (orthogonal) transformation

$$\begin{pmatrix} \tilde{\phi}_1 \\ \tilde{\phi}_2 \end{pmatrix} = \hat{U} \begin{pmatrix} \phi_1 \\ \phi_2 \end{pmatrix} \equiv \begin{pmatrix} \cos \theta & \sin \theta \\ -\sin \theta & \cos \theta \end{pmatrix} \begin{pmatrix} \phi_1 \\ \phi_2 \end{pmatrix}, \quad (44)$$

where θ is the rotation angle. Clearly, the creation and annihilation operators corresponding to each set of the orbitals are coupled via \hat{U} as well:

$$\begin{pmatrix} \tilde{b}_1^{(\dagger)} \\ \tilde{b}_2^{(\dagger)} \end{pmatrix} = \begin{pmatrix} \cos \theta & \sin \theta \\ -\sin \theta & \cos \theta \end{pmatrix} \begin{pmatrix} b_1^{(\dagger)} \\ b_2^{(\dagger)} \end{pmatrix}. \quad (45)$$

Since all possible real MCHB(2) orbitals can be obtained from the initial (ϕ_1, ϕ_2) ones by changing the angle θ , the respective distributions of the expansion coefficients as well as their mean values and variances depend also on this angle. Here we are interested in the variance:

$$\tilde{\sigma}_{n_1}^2 \equiv \langle \tilde{n}_1^2 \rangle - \langle \tilde{n}_1 \rangle^2 = \langle \tilde{b}_1^\dagger \tilde{b}_1 \tilde{b}_1^\dagger \tilde{b}_1 \rangle - \langle \tilde{b}_1^\dagger \tilde{b}_1 \rangle^2 = \sigma^2(\theta). \quad (46)$$

After straightforward algebra one finds

$$\begin{aligned} \sigma^2(\theta) &= \cos^4 \theta (\langle \hat{n}_1^2 \rangle - \langle \hat{n}_1 \rangle^2) + \sin^4 \theta (\langle \hat{n}_2^2 \rangle - \langle \hat{n}_2 \rangle^2) \\ &+ \sin^2 \theta \cos^2 \theta [4 \langle \hat{n}_1 \hat{n}_2 \rangle - 2 \langle \hat{n}_1 \rangle \langle \hat{n}_2 \rangle + N + \rho_{1122} + \rho_{2211} - (\rho_{12} + \rho_{21})^2] \\ &+ 2 \sin \theta \cos^3 \theta [\rho_{12} + \rho_{1112} + \rho_{2111} - (\rho_{12} + \rho_{21}) \langle \hat{n}_1 \rangle] \\ &+ 2 \sin^3 \theta \cos \theta [\rho_{21} + \rho_{1222} + \rho_{2221} - (\rho_{12} + \rho_{21}) \langle \hat{n}_2 \rangle], \end{aligned} \quad (47)$$

where the involved diagonal and off-diagonal elements of the reduced one- and two-body density matrices are given in Eqs.(22,23) and in Appendix A. The extrema of this function are obtained in the ordinary way, by solving

$$\frac{\partial}{\partial \theta} \sigma^2(\theta) = 0. \quad (48)$$

The procedure of finding the distribution with minimal variance is implemented as follows. Having at hand a MCHB(2) solution, i.e., the orbitals (ϕ_1, ϕ_2) and a set of the respective expansion coefficients $\{C_{(n_1, n_2)}\}$, we recompute all required elements of the reduced one- and two-body density matrices, appearing in Eq.(47) and explicitly reconstruct the variance $\sigma^2(\theta)$. The angle θ_{min} at which this function has a minimum is obtained numerically by solving Eq.(48). The unitary transformation Eq.(44) with this angle gives a new set of MCHB(2) orbitals $(\tilde{\phi}_1, \tilde{\phi}_2)$. The distribution of expansion coefficients computed on these orbitals has the minimal variance σ_{min} . Obviously, we can call such a distribution the *minimal* distribution.

The natural orbitals being the MCHB solutions can be used to shed light on the physical nature (depletion or fragmentation) of the ground and excited states. Let us see how the expansion coefficients distributions of the many-body basis sets constructed by using the natural orbitals look like. In the left lower panel of Fig.5 we plot the expansion coefficients obtained for the ground state of $N=1000$ bosons with $\lambda_0 = 0.01$ trapped in the symmetric double-well potential Eq.(40). This system has been discussed above in Sec.III B. The

corresponding ground state natural orbitals are very similar to those plotted in the right lower panel of Fig.6. Due to the symmetry of the trap potential, the ground many-body state is, of course, of gerade symmetry, while the natural orbitals are of gerade and ungerade symmetries. Therefore, for the ground state the non-zero expansion coefficients can appear only due to the contributions of configurations of gerade symmetry. Indeed, in the left lower panel of Fig.5 one can see that the configurations with even number of bosons residing in the ungerade orbital contribute, while those with odd numbers i.e., $|1000 - 1, 1\rangle$, $|1000 - 3, 3\rangle$, $|1000 - 5, 5\rangle$ etc., give zero contributions. In this figure it is clearly seen that the main contributions come from the first configurations, where almost all bosons reside in the first orbital, while the configurations with large populations of the second orbital do not contribute. This observation is supported by the statistical description of this distribution in terms of its mean values (see Eq.(43)). The mean statistical values of this distribution are $\nu_1 = \langle \hat{n}_1 \rangle = 994.78$ and $\nu_2 = \langle \hat{n}_2 \rangle = 5.22$. As one would expect these mean values are identical to the natural occupation numbers of the respective natural orbitals.

In the right lower panel of Fig.5 we plot the expansion coefficients obtained for the system of $N=1000$ bosons with $\lambda_0 = 0.01$ trapped in the asymmetric double-well potential Eq.(41) discussed in Sec.III C. The corresponding natural orbitals presented in the right upper panel of Fig.4 do not possess any symmetry. Consequently, all the many-body basis functions constructed by using these natural orbitals can give non-zero contributions in the many-body expansion. Indeed, we can see this in the right lower panel of Fig.5. The mean statistical values of this asymmetric distribution $\nu_1 = \langle \hat{n}_1 \rangle = 906.06$ and $\nu_2 = \langle \hat{n}_2 \rangle = 93.94$ are, of course, identical to the respective natural orbital occupation numbers.

Let us see how the variance $\sigma_{n_1}^2 = \langle \hat{n}_1^2 \rangle - \langle \hat{n}_1 \rangle^2$ characterizes the distributions of the expansion coefficients. Inspecting the distributions obtained with natural orbitals we see in the lower panels of Fig.5 that for the symmetric double-well, where only several many-body basis function have non-zero expansion coefficients, the variance is quite small $\sigma_{NO} = 7.654$. While in the asymmetric case, where almost all expansion coefficients have non-zero contributions, the width of the distribution is much larger $\sigma_{NO} = 121.731$. We conclude that the value of the statistical variance σ^2 , characterizing the width of the distribution of the expansion coefficients, indeed provides an adequate estimation on the number of contributing configurations.

Now let us see how the minimal distributions, i.e., the distributions with minimal width

look like. We consider the same examples of the symmetric and asymmetric double-wells as above, and find their minimal distributions by using the developed algorithm (see Eq.(48)). The minimal distributions obtained for the symmetric and asymmetric double-wells are presented in the left and right upper panels of Fig.5 respectively. The respective variances are also depicted. The minimal distribution obtained for the symmetric double-well trap has a maximum located exactly at the $|500, 500\rangle$. This is a symmetric distribution because the pairs of basis vectors around maximum $|500 - i, 500 + i\rangle$ and $|500 + i, 500 - i\rangle$ contribute with identical coefficients. Interestingly, the minimal distribution is smooth, in contrast to that obtained within the natural orbitals, where the neighboring MCHB(2) coefficients are of different sign, see lower left panel of Fig.5. The width of the minimal distribution is, of course, smaller than that for the natural orbital, $\sigma_{min} = 3.313$ in comparison to $\sigma_{NO} = 7.654$.

Comparing the right upper and lower panels of Fig.5 we see that in the presented example of asymmetric double-well trap the minimal distribution differs substantially from that obtained within the natural orbitals. For the asymmetric case, the width of the minimal distribution $\sigma_{min} = 0.753$ is about 2.5 orders of magnitude smaller than that for the natural orbital $\sigma_{NO} = 121.731$. This means that the minimal distribution is formed by several configurations in contrast to the broad distribution obtained with natural orbitals where all configurations contribute. The maximum of the minimal distribution is located around $|600, 400\rangle$. The distribution is smooth and, of course, not symmetric.

Irrespective of the symmetry of the trap potential used, the width of the minimal distribution can be much smaller than that obtained with the natural orbitals. The profile of the minimal distribution is smooth, while the distribution of the expansion coefficients obtained within other orbital sets is not necessarily so. These observations lead to several important consequences. First, the minimal distribution of the expansion coefficients can be approximated by a smooth continuous function. Looking at the pictures in Fig.5 we approximate the probability function Eq.(42) of the minimal distribution by a Gaussian function:

$$P(\xi) = \frac{1}{\sqrt{2\pi}\sigma} \exp \frac{-(\xi - \xi_0)^2}{2\sigma^2}. \quad (49)$$

The parameters of this function are obtained straightforwardly. We take $\xi = n_1$ as an independent variable. The averages Eq.(43) of the minimal distribution define the location $\xi_0 = \langle \hat{n}_1 \rangle$ and width $\sigma = \sigma_{min}$ of the Gaussian. In the upper panels of Fig.5 we plot the Gaussian distribution functions approximating the minimal distributions of the studied

symmetric and asymmetric systems by black solid lines. We stress that in Fig.5 we plot the distributions of the expansion coefficients, i.e., $\sqrt{P(n_1)}$. In this figure we see that the Gaussian distributions match the numerical results very well. Moreover, once a MCHB calculation has been performed, this continuous Gaussian approximation does not require any fitting parameters.

We mention that continuous approximations to the discrete distributions of the expansion coefficients have already been addressed in the literature for symmetric trap potentials [30, 40]. In these studies *smoothness* of the real CI coefficients and thus of the continuum distribution approximation was used as a basic *assumption*. In contrast, here we have demonstrated numerically that the profile of the distribution of the expansion coefficients obtained within MCHB many-body method can indeed be smooth. Moreover, the smooth profiles of the discrete distribution of the expansion coefficients are observed in examples of symmetric as well as of asymmetric trap potentials. However, it is very important to stress that smoothness is achieved only for the minimal distributions, i.e., for a very specific choice of the orbitals (see Eq.(47)).

Finally, we remark that the existence of smooth continuous functions approximating the discrete distribution of the expansion coefficients makes the developments of self-consistent many-body methods very promising for attacking many-particle bosonic systems within huge configurational spaces.

E. Excited states in 1D symmetric double-well trap

In the preceding sections we considered the ground state of a trapped bosonic system and addressed condensation and fragmentation as properties of the ground state. The main subject of this part of our work is to touch upon properties of excited states of trapped bosons. The studies on excited states are of great interest [12, 13, 14, 15, 38] because of their relevance for depletion and stability of condensates, for time-dependent and finite-temperature effects, for formations of solitons and soliton trains [39], as well as for other interesting phenomena.

Let us assume that we have obtained the self-consistent MCHB orbitals for the ground state of the bosonic system. Since in the MCHB scheme the diagonalization of the secular matrix was employed we also have the energies and many-body wave-functions of the excited

states. However, the excited states computed in this way are *not* self-consistent. Here we address the question whether the self-consistent orbitals obtained for the ground state can also be used to provide an adequate description of the excited states or whether every excited state has to be treated individually.

To answer this question we consider a system of $N=1000$ bosons with $\lambda_0 = 0.01$ trapped in a symmetric double-well potential. In this example we use the trap:

$$V_{symm}(x) = 0.5x^2 - \frac{1}{2}\sqrt{25 + 64x^2} + V_b(A = 25, D = 0.75) + 8.19523,$$

obtained by diagonalizing Eq.(38) with $V_1(x) = 0.5(x+4.0)^2$, $V_2(x) = 0.5(x-4.0)^2$, $C = 2.5$, $B = 0.0$ and by adding a barrier function $V_b(A = 25, D = 0.75)$. To put the minimum of the potential energy to zero we also use a constant shift.

First, we apply the MCHB(2) approach to obtain the self-consistent energy and orbitals of the ground state. This state is essentially condensed because the occupation numbers of the corresponding reduced one-particle density matrix are $\rho_1 = 994.78$ and $\rho_2 = 5.22$. In other words, 994.78 particles are condensed in the first natural orbital and 5.22 are excited out to the second orbital. The density and respective natural orbitals are plotted in the lower right panel of Fig.6. We recall that the natural orbitals are solutions of the MCHB.

Having at hand the self-consistent ground state orbitals we diagonalize the full secular matrix and get the energies of the excited states. In the left panel of Fig.6 we depict the energy level of the first excited state. We connect both levels by a vertical solid line with arrow to stress that this first excited state is obtained by using the MCHB orbitals of the ground state. The natural orbital analysis applied reveals that the occupations numbers of this first excited state are $\rho_1 = 985.20$, $\rho_2 = 14.80$ and the natural orbitals of this excited state are almost identical to the ground state ones. Comparing the natural orbital occupation numbers of the ground and this first excited state we conclude that this excited state can be considered as a further microscopic excitation of a small number of particles out of the condensate, i.e., a further depletion of the condensate.

Let us now see what happens when the first excited state is treated self-consistently. To realize this we employ the developed MCHB(2) method to the excited states as follows. We recall that in our iterative MCHB scheme the many-body expansion coefficients corresponding to the ground state are obtained as components of the first, i.e., lowest-energy eigenvector of the secular matrix. To attack the first excited state we use the components of

the second eigenvector during all iterations. The self-consistent results obtained by applying this procedure to the first excited state are also depicted in Fig.6 and marked as "SC Excited State". The natural orbitals and the density corresponding to this state are shown in the upper right panel and its energy level is depicted in the left panel.

From Fig.6 it is clearly seen that self-consistency can have an enormous impact on properties of an excited state. The energy of the first excited state obtained self-consistently is much lower than that obtained by using the ground state orbitals. The self-consistent first excited state is almost 30% fragmented. The respective natural orbital occupation numbers are $\rho_1 = 734.84$ and $\rho_2 = 265.16$, contrasting $\rho_1 = 985.20$ and $\rho_2 = 14.80$ obtained above for the non-self-consistent excited state. By comparing the upper and lower right panels of Fig.6 we see that the shapes of the first natural orbitals (red) in both calculations are almost identical, while those of the second natural orbitals (blue) differ drastically from each other. Moreover, it is easily seen in the right upper panel of Fig.6 that a simple linear combination of the natural orbitals of the first self-consistent excited state gives almost pure left and right localized functions, which are, of course, solutions of the MCHB as well. For the ground state orbitals depicted in the right lower panel of Fig.6 such a localized presentation can not be obtained. From this analysis we conclude that the first self-consistent excited state and the ground state are qualitatively different and exhibit a different "topology".

In this example the ground state of the system is condensed and the first excited state is fragmented. Fragmentation is shown to be much more favorable energetically than a further depletion of the condensate. One goal of this study is to demonstrate that self-consistency can be very important for an adequate description of excited states. Indeed, we have shown that without self-consistency the lowest-energy excited state describes a depletion of the condensate. The inclusion of self-consistency significantly lowers the energy of the first excited state and drastically changes its character. Instead of depletion of the condensate it describes its fragmentation. We stress that excited states of different topology also exist in many other trapped bosonic systems. The question whether they are low-lying or highly excited states depends on trap geometries, number of particles and strength of inter-particle interaction.

F. Ground state in 2D symmetric double-well trap

In the present section we investigate the relevance of self-consistency for many-body studies on trapped bosonic systems in higher dimensions. For illustration, here we investigate a repulsive bosonic system trapped in the two-dimensional symmetric double-well potential

$$V_{symm}(x, y) = 0.5x^2 + 0.5y^2 - \frac{1}{2}\sqrt{25 + 64x^2} + 8.19531 + V_b(A = 8, D = 0.75). \quad (50)$$

This potential is obtained according to Eq.(38) as a superposition of two pure harmonic 2D potentials $V_1(x, y) = 0.5[(x + 4.0)^2 + y^2]$ and $V_2(x, y) = 0.5[(x - 4.0)^2 + y^2]$ with $C = 2.5$, $B = 0.0$ and by adding the two-dimensional barrier function $V_b(A, D) = \frac{4}{\sqrt{2\pi D}} \exp[-(x + y)^2/(2D^2)]$. Here, we have also applied a constant shift to put the minimum of the potential energy to zero.

The ground state of $N=1000$ identical bosons at $\lambda_0 = 0.01$ trapped in this double-well trap has been investigated within the framework of the fixed-orbital and self-consistent MCHB(2) many-body methods. The two eigenfunctions lowest in energy of the respective two dimensional bare Hamiltonian Eq.(37) have been used to construct the fixed-orbital many-body basis set. As in the one-dimensional case, we use these functions as an initial guess for solving MCHB(2) equations.

The geometry of the double-well trap used implies that the ground state density is made of two parts each localized in one well. Due to the perfect two-fold symmetry of the trap potential it suffices to consider only one of them without loss of information. In Fig.7, for convenience of comparison, we depict the part of the self-consistent MCHB(2) ground state density localized in the left well together with the part of the total density obtained within the usual fixed-orbital many-body method localized in the right well. From this figure it is clearly seen that the densities obtained are very different. To better account for the repulsion between the bosons, the self-consistent density is more delocalized within the well than the fixed orbital one. Of course, the MCHB(2) solution has a lower energy than the fixed orbital one. The natural orbital analysis applied shows that in the MCHB(2) case $\rho_1 = 750$ bosons reside in one orbital and $\rho_2 = 250$ bosons in the other orbital, while for the many-body solution obtained with fixed bare Hamiltonian orbitals these occupations are $\rho_1 = 634$ and $\rho_2 = 366$. Both many-body methods give the same qualitative prediction on the nature of the ground state – this state is fragmented, however, the predicted details of

the fragmentation are very different.

In this investigation we have demonstrated that analogously to the 1D case, self-consistency is of great relevance for the many-body description of bosonic systems in higher dimensions.

IV. IMPLEMENTATION OF THE MCHB(M) FOR TWO BOSONS IN A TRAP

The technical realization of the developed MCHB method for the general case of M orbitals and N bosons requires considerable methodological and algorithmical efforts. In this section we perform the first step in this direction and implement the MCHB(M) theory for two interacting bosons.

We consider a system of two bosons interacting via contact inter-particle potential trapped in the 1D symmetric double-well potential

$$V_{symm}(x) = 0.5x^2 - 2.5\sqrt{0.0784 + x^2} + 3.16204 + V_b(A = 1, D = 0.75). \quad (51)$$

To obtain this potential we take the lowest-energy eigenvalue of Eq.(38) with $V_1(x) = 0.5(x + 2.5)^2$, $V_2(x) = 0.5(x - 2.5)^2$, $C = 0.7$, $B = 0.0$ and add a barrier function $V_b(A = 1, D = 0.75)$. The minimal value of this potential energy has been adjusted to zero by applying a constant shift.

In Fig.8 we plot the ground state energy of this system as a function of the inter-particle interaction strength λ_0 , obtained within the framework of the self-consistent many-body MCHB(M) method, $M=2, \dots, 10$. We also present the energies obtained within one- and two-orbital mean-fields, MF(1) and MF(2) respectively. All the energies are plotted with respect to the ground state energy $E(0)$ of the non-interacting two-boson system. At this limit the ground state many-body wave-function is given by a single configuration where both bosons reside in the lowest-energy orbital of the respective bare Hamiltonian, and the total energy of this ground state $E(0)$ is twice the respective orbital energy.

In this figure it is very difficult to distinguish between the energy curves obtained within the two-orbital MCHB(2) theory and the multi-orbital MCHB(M) $M=3, \dots, 10$ ones. This observation tells us that for our example an adequate description can already be obtained within the two-orbital MCHB(2) method, the inclusion of more orbitals does not lead to significant "observable" improvements. We demonstrate this in the inset of Fig.8, where

we present a part of the MCHB(M) energy curves on an enlarged scale. Comparing the energy gaps between successive MCHB(M) energy curves, we observe the convergence of the MCHB(M) method.

To arrive at a deeper insight into the role of many-body effects we also study the trapped two-bosonic system within the framework of multi-orbital mean-field theory which is a limiting one-permanent case of the MCHB approach as we have shown in Sec.II C. We recall that the one-orbital mean-field MF(1) is the famous Gross-Pitaevskii mean-field. In Fig.8 the MF(1) energy curve is depicted by a dashed line. The one-orbital mean-field solution describes a "condensate" where both bosons reside in the same orbital. The two-orbital mean-field MF(2) solution describes a situation where one boson resides in one orbital and the second boson occupies another orbital. For the two-boson system such a state can be considered as a two-fold "fragmented" state. Here we observe a "critical phenomenon". Up to some critical value of the inter-particle interaction strength the "condensed" solution is energetically more favorable than the "fragmented" one. From this critical λ_0 on, the ground state becomes two-fold "fragmented". The intersection of the MF(1) and MF(2) energy curves gives the critical interaction strength at $\lambda_0 = 0.0203$. In Fig.8 we mark this point by a cross.

The MCHB theory gives the following many-body picture of this transition. The natural orbital analysis applied to the MCHB(M) solutions at each λ_0 reveals that the character of the many-body MCHB(M) ground state smoothly develops with inter-particle interaction strength from "condensed", where only one natural orbital is occupied, to the two-fold "fragmented" where two natural orbital have dominant and nearly equal occupations. Having at hand the natural orbital occupation numbers as a function of λ_0 , we find the inflection point at $\lambda_0 = 0.0142$ and attribute it to the transition point. In Fig.8 this point is marked by a bold filled circle. The comparison between many-body and mean-field predictions shows that in contrast to the sharp transition obtained within the multi-orbital mean-fields, an inclusion of the many-body effect makes this transition smooth, i.e., it is a crossover.

This investigation of the minimal many-body system has verified that qualitative predictions on the transition from condensation to fragmentation in symmetric double wells can already be obtained within the framework of the self-consistent multi-orbital mean-field theory [20, 21, 22]. We also demonstrated that the two-orbital MCHB(2) theory provides in this case an accurate quantitative description and the inclusion of more orbitals leads to

minor changes. Generally, MCHB(M) opens the door to treat any two-boson system.

V. DISCUSSION AND CONCLUSIONS

In this work we developed a complete variational many-body theory for systems of N trapped bosons interacting via a general two-body interaction potential. The many-body wave function of this system is expanded over orthogonal many-body basis functions (configurations). Each basis function is constructed as a symmetrized Hartree product (permanent) with N bosons distributed over M one-particle functions. These one-particle functions *and* the respective expansion coefficients are treated as the variational parameters in this theory. The optimal variational parameters are obtained *self-consistently* by solving a coupled system of non-eigenvalue integro-differential equations to get the one-particle functions and, by diagonalizing the secular Hamiltonian matrix problem, to find the expansion coefficients. To construct this matrix we derived *general* rules for matrix elements, which are of relevance also for other many-body theories. We call this self-consistent theory multi-configurational Hartree for bosons, or MCHB(M) where M specifies the number of one-particle functions involved.

The properties of the MCHB(M) equations were discussed. These equations are formally also valid for any size of the many-body expansion, i.e., for any number of configurations used in the expansion. Therefore, the MCHB(M) theory allows to find also the best possible many-body solution within any restricted configurational space used. We have shown that in the limiting case where only one permanent forms the many-body expansion, the MCHB(M) theory boils down to the self-consistent mean fields. In the simplest case when all bosons reside in the same orbital one gets the Gross-Pitaevskii equation. The multi-orbital mean-field theory is obtained in the more general single-permanent case, when bosons are allowed to reside in several one-particle functions.

We have shown that if the many-body basis set spans a complete subspace of the Hilbert space, namely, when all possible configurations appearing as permutations of N bosons over M orbitals are taken into account, then the MCHB(M) solution is invariant with respect to a unitary transformation (linear combination) of the MCHB(M) orbitals. This property has been used to demonstrate that eigenfunctions of the reduced one-particle density, i.e., the natural orbitals are the MCHB(M) solution as well. We proposed to analyze the ground

and excited states in the terms of the natural orbitals and natural occupation numbers to more easily identify the depletion and fragmentation of the condensates.

In the second part of our work we implemented the MCHB(M) method with $M=2$ orbitals. We applied it to study the ground and excited states of the bosonic systems with the popular contact inter-particle interaction trapped in one- and two-dimensional symmetric and asymmetric double-well traps. The considered configurational space was spanned by all possible permutations of $N=1000$ bosons over two orbitals. Two lowest-energy eigenfunctions of the respective bare Hamiltonian were used to construct the often employed fixed-orbital many-body basis set. We compare the fixed-orbital many-body predictions with those obtained self-consistently via the MCHB(2) theory to investigate the impact and relevance of self-consistency.

We performed several ground state studies of the bosonic system trapped in the symmetric double-well trap. In the first study, we keep the shape of the symmetric double-well trap potential fixed and vary the strength λ_0 of the inter-particle interaction in order to study the ground state fragmentation. We have seen that self-consistent MCHB(2) theory predicts a gradual enhancement of the fragmented fraction with λ_0 up to some critical inter-particle interaction strength, where the fragmentation achieves its maximal value. Further increase of λ_0 causes gradual decreasing of the fragmentation, because the energy of the bosonic system in this regime becomes larger than the potential barrier. The many-body result obtained within fixed bare Hamiltonian functions predicts a gradual enhancement of the fragmentation with increasing λ_0 followed by an unphysical saturation of the fragmented fraction to some constant value. In the second study, to investigate the transition point from condensation to fragmentation we keep the inter-particle interaction strength fixed and rump the barrier up. The critical value of the barrier height obtained with bare Hamiltonian functions are considerably underestimated in comparison with the more exact, self-consistent, MCHB(2) many-body predictions. A main conclusion derived from this investigation is that the quantitative characterization of the ground state properties of the bosonic system trapped in symmetric double-wells can be obtained in the framework of self-consistent methods, the fixed-orbital many-body theory utilizing the same size of CI expansion can be unreliable even concerning qualitative predictions.

We addressed the ground state properties of the bosonic system trapped in the asymmetric double-well potential. In this study we keep the shape of the asymmetric double-well trap

potential fixed and vary the strength of the inter-particle interaction. The MCHB(2) theory predicts two regimes for the ground state. In the first one the atomic cloud is localized in the deeper well; from some critical inter-particle interaction strength on the system enters the second regime where bosons occupy both wells. We show that such a picture can not be obtained within a fixed two-orbital many-body treatment. To overcome this difficulty, one must use at least three fixed orbitals to construct the permanents. However the active space, i.e., the number of many-body basis functions used in this case is substantial and often beyond reach.

To exploit the freedom of unitary transformations we analyzed the distribution of the MCHB(2) expansion coefficients obtained for different linear combinations of the MCHB(2) orbitals for the ground state of the bosonic systems trapped in the symmetric and asymmetric double-wells. We verified that statistical means and variances can indeed be used to characterize adequately the distributions of the expansion coefficients. Moreover, we have seen that the distributions with minimal width, obtained by minimizing the variance, exhibit very smooth profiles, irrespective of the symmetry of the trap potential used. For the studied examples the profiles of the smooth minimal distributions can very well be approximated by continuous Gaussian functions.

We also investigated the first excited state of the system trapped in the symmetric double-well and demonstrate that self-consistency can be very important for an adequate description of excited states. We used the natural orbitals analysis to classify the ground and excited states. It was shown that without self-consistency the lowest-energy excited state describes a depletion of the condensate. The inclusion of self-consistency significantly lowers the energy of the first excited state and on top of that drastically changes its character: Instead of describing a condensate with a slightly larger depleted fraction, it describes a fragmented condensate with a substantial degree of almost 30% fragmentation.

As an illustrative example we investigate the ground state of a two dimensional bosonic system trapped in a symmetric double-well potential. We show that self-consistency is expected to be of high relevance for many-body studies on trapped bosonic systems also in higher dimensions.

Finally, we have shown that the two-orbital MCHB(2) theory can provide quite accurate quantitative description for the ground state of two-bosonic systems in symmetric double-well traps. The MCHB(M) has been implemented for two bosons and in an illustrative

example the inclusion of more orbitals leads only to minor changes.

APPENDIX A: OFF-DIAGONAL ELEMENTS OF TWO-BODY DENSITY MATRIX

In this appendix we evaluate the off-diagonal elements of the two-body density matrix $\rho_{ijkl} = \langle \Psi | b_i^\dagger b_j^\dagger b_k b_l | \Psi \rangle$. We use the same shorthand notations as defined in Sec.II B 1 where only occupation numbers of the involved orbitals are shown. For instance, the configuration $(; n_i - 2; n_j + 2;)$ differs from $\vec{n} \equiv (; n_i; n_j;)$ by excitation of two bosons from ϕ_i to ϕ_j . In all cases different indices can not have the same value.

$$\begin{aligned} \rho_{iijj} &= \sum_{\vec{n}} C_{\vec{n}}^* C_{(;n_i-2;n_j+2;)} \sqrt{n_i(n_i-1)(n_j+1)(n_j+2)}, \\ \rho_{iijk} &= \sum_{\vec{n}} C_{\vec{n}}^* C_{(;n_i-2;n_j+1;n_k+1;)} \sqrt{n_i(n_i-1)(n_j+1)(n_k+1)}, \\ \rho_{ijkl} &= \sum_{\vec{n}} C_{\vec{n}}^* C_{(;n_i-1;n_j-1;n_k+1;n_l+1;)} \sqrt{n_i n_j (n_k+1)(n_l+1)}, \\ \rho_{ijkk} &= \sum_{\vec{n}} C_{\vec{n}}^* C_{(;n_i-1;n_j-1;n_k+2;)} \sqrt{n_i n_j (n_k+1)(n_k+2)}, \\ \rho_{iijj} &= \sum_{\vec{n}} C_{\vec{n}}^* C_{(;n_i-1;n_j+1;)} (n_i-1) \sqrt{n_i(n_j+1)}, \\ \rho_{ijjj} &= \sum_{\vec{n}} C_{\vec{n}}^* C_{(;n_i-1;n_j+1;)} n_j \sqrt{n_i(n_j+1)}, \\ \rho_{ikkk} &= \sum_{\vec{n}} C_{\vec{n}}^* C_{(;n_i-1;n_j+1;)} n_k \sqrt{n_i(n_j+1)}. \end{aligned}$$

All other matrix elements are zero or can be reduced to the above ones due to symmetries of the two-body operator:

$$\rho_{ijkl} = \rho_{jikl} = \rho_{ijlk} = \rho_{jilk}.$$

When the many-body function $|\Psi\rangle$ and one-particle orbitals are real functions, some additional symmetries are implied: $\rho_{12} = \rho_{21}$, $\rho_{2111} = \rho_{1112}$ $\rho_{2221} = \rho_{1222}$ and $\rho_{2211} = \rho_{1122}$.

ACKNOWLEDGMENTS

We acknowledge stimulating discussions with J. Schmiedmayer and M. Oberthaler.

-
- [1] M.H. Anderson, J.R. Ensher, M.R. Matthews, C.E. Wieman, and E.A. Cornell, *Science* **269**, 198 (1995).
- [2] K.B. Davis, M.-O. Mewes, M.R. Andrews, N.J. van Druten, D.S. Durfee, D.M. Kurn, and W. Ketterle, *Phys. Rev. Lett.* **75**, 3969 (1995).
- [3] C.C. Bradley, C.A. Sackett, J.J. Tollett, and R.G. Hulet, *Phys. Rev. Lett.* **75**, 1687 (1995).
- [4] J. Reichel, W. Hänsel, and T.W. Hänsch, *Phys. Rev. Lett.* **83**, 3398 (1999).
- [5] P. Krüger, X. Luo, M.W. Klein, K. Brugger, A. Haase, S. Wildermuth, S. Groth, I. Bar-Joseph, R. Folman, and J. Schmiedmayer, *Phys. Rev. Lett.* **91**, 233201 (2003).
- [6] R. Dumke, T. Müther, M. Volk, W. Ertmer, and G. Birkl, *Phys. Rev. Lett.* **89**, 220402 (2002).
- [7] C.-S. Chuu, F. Schreck, T.P. Meyrath, J.L. Hanssen, G.N. Price, and M.G. Raizen, *Phys. Rev. Lett.* **95**, 260403 (2005).
- [8] A. Marte, T. Volz, J. Schuster, S. Dürr, G. Rempe, E.G.M. van Kempen, and B.J. Verhaar, *Phys. Rev. Lett.* **89**, 283202 (2002).
- [9] M. Albiez, R. Gati, J. Fölling, S. Hunsmann, M. Cristiani, and M.K. Oberthaler, *Phys. Rev. Lett.* **95**, 010402 (2005).
- [10] Y. Shin, M. Saba, T.A. Pasquini, W. Ketterle, D.E. Pritchard, and A.E. Leanhardt, *Phys. Rev. Lett.* **92**, 050405 (2004).
- [11] T. Schumm, S. Hofferberth, L.M. Andersson, S. Wildermuth, S. Groth, I. Bar-Joseph, J. Schmiedmayer, P. Krüger, *Nature Physics* **1**, 57 (2005).
- [12] A.S. Parkins and D.F. Walls, *Phys. Rep.* **303**, 1 (1998).
- [13] F. Dalfovo, S. Giorgini, L.P. Pitaevskii, and S. Stringari, *Rev. Mod. Phys.* **71**, 463 (1999).
- [14] A.J. Leggett, *Rev. Mod. Phys.* **73**, 307 (2001).
- [15] L. Pitaevskii, S. Stringari, *Bose-Einstein Condensation*, (Oxford Univ. Press, London, 2003).
- [16] E.H. Lieb and W. Liniger, *Phys. Rev.* **130**, 1605 (1963); J.G. Muga and R.F. Snider, *Phys. Rev. A* **57**, 3317 (1998); K. Sakmann, A.I. Streltsov, O.E. Alon and L.S. Cederbaum, *ibid.* **72**, 033613 (2005).
- [17] M. Gaudin, *Phys. Rev. A* **4**, 386 (1971); M.T. Batchelor et al., *J. Phys. A: Math. Gen.* **38**, 7787 (2005).
- [18] T. Busch et al., *Found. Phys.* **28**, 549 (1998); M.A. Cirone et al., *J. Phys. B: At. Mol. Opt.*

- Phys.* **34**, 4571 (2001).
- [19] E.P. Gross, *Nuovo Cimento* **20**, 454 (1961); L.P. Pitaevskii, *Zh. Eksp. Teor. Fiz.* **40**, 646 (1961); L.P. Pitaevskii, *Sov. Phys. JETP* **13**, 451 (1961).
- [20] L.S. Cederbaum and A.I. Streltsov, *Phys. Lett. A* **318**, 564 (2003).
- [21] A.I. Streltsov and L.S. Cederbaum, *Phys. Rev. A* **71** 063612 (2005).
- [22] O.E. Alon, A.I. Streltsov and L.S. Cederbaum, *Phys. Lett. A* **347**, 88 (2005).
- [23] O.E. Alon and L.S. Cederbaum, *Phys. Rev. Lett.* **95**, 140402 (2005).
- [24] O.E. Alon, A.I. Streltsov, and L.S. Cederbaum, *Phys. Rev. Lett.* **95**, 030405 (2005).
- [25] A. Szabo and N.S. Ostlund, *Modern Quantum Chemistry* (Dover, Mineola, NY, 1996).
- [26] R. Kanamoto, H. Saito, and M. Ueda, *Phys. Rev. A* **67**, 013608 (2003); R. Kanamoto, H. Saito, and M. Ueda, *ibid.* **A 68**, 043619 (2003); T. Nakajima and M. Ueda, *Phys. Rev. Lett.* **91** 140401 (2003); R. Kanamoto, H. Saito, and M. Ueda, *ibid.* **94** 090404 (2005).
- [27] T. Haugset and H. Haugerud, *Phys. Rev. A* **57**, 3809 (1998).
- [28] G.F. Bertsch and T. Papenbrock, *Phys. Rev. Lett.* **83**, 5412 (1999); N.R. Cooper, N.K. Wilkin, and J.M.F. Gunn, *ibid.* **87**, 120405 (2001); M.A.H Ahsan and N. Kumar, *Phys. Rev. A* **64**, 013608 (2001); X. Liu, H. Hu, L. Chang, and S.-Q. Li, *ibid.* **64**, 035601 (2001); D.J. Dean and T. Papenbrock, *ibid.* **65**, 043603 (2002); M. Toreblad, M. Borgh, M. Koskinen, M. Manninen, and S.M. Reimann, *Phys. Rev. Lett.* **93**, 090407 (2004).
- [29] O.E. Alon, A.I. Streltsov, K. Sakmann and L.S. Cederbaum, *Europhys. Lett.* **67**, 8 (2004).
- [30] R.W. Spekkens and J.E. Sipe, *Phys. Rev. A* **59**, 3868 (1999).
- [31] D. Masiello, S.B. McKagan, and W.P. Reinhardt, *Phys. Rev. A* **72**, 063624 (2005).
- [32] O. Penrose and L. Onsager, *Phys. Rev.* **104**, 576 (1956).
- [33] P. Nozieres and D. Saint James, *J. Phys. (Paris)* **43**, 1133 (1982); P. Nozieres, in *Bose-Einstein Condensation*, edited by A. Griffin, D.W. Snoke, and S. Stringari (Cambridge University Press, Cambridge, England, 1996).
- [34] K.W. Mahmud, J.N. Kutz, and W.P. Reinhardt, *Phys. Rev. A* **66**, 063607 (2002) ; M.W. Jack, M.J. Collett, and D.F. Walls, *ibid.* **54**, R4625 (1996); J. Javanainen, *ibid.* **54**, R4629 (1996); J. Ruostekoski and D.F. Walls, *ibid.* **58**, R50 (1998); S. Raghavan, A. Smerzi, S. Fantoni and S.R. Shenoy, *ibid.* **59**, 620 (1999); L. Pitaevskii and S. Stringari, *Phys. Rev. Lett.* **87**, 180402 (2001); G.L. Salmond, C.A. Holmes, and G.J. Milburn, *Phys. Rev. A* **65**, 033623 (2002).
- [35] D. Ananikian and T. Bergeman, *Phys. Rev. A* **73**, 013604 (2006).

- [36] E. Sakellari, M. Leadbeater, N.J. Kylstra, and C.S. Adams, Phys. Rev. A **66**, 033612 (2002); M. Jääskeläinen and P. Meystre, Phys. Rev. A **73**, 013602 (2006).
- [37] M. Girardeau, J. Math. Phys. (N.Y.) **1**, 516 (1960); T. Kinoshita et al., Science **305**, 1125 (2004); B. Paredes et al., Nature (London) **429**, 277 (2004).
- [38] R. Ozeri, N. Katz, J. Steinhauer, and N. Davidson, Rev. Mod. Phys. **77**, 187 (2005).
- [39] S. Burger et al., Phys. Rev. Lett. **83**, 5198 (1999); J. Denschlag et al., Science **287**, 97 (2000); L. Khaykovich et al., Science **296**, 1290 (2002); K.E. Strecker et al., Nature (London) **417**, 150 (2002); B. Eiermann et al., Phys. Rev. Lett. **92**, 230401 (2004).
- [40] J. Javanainen and M.Yu. Ivanov, Phys. Rev. A **60**, 2351 (1999); J. Javanainen, *ibid.* **60**, 4902 (1999).

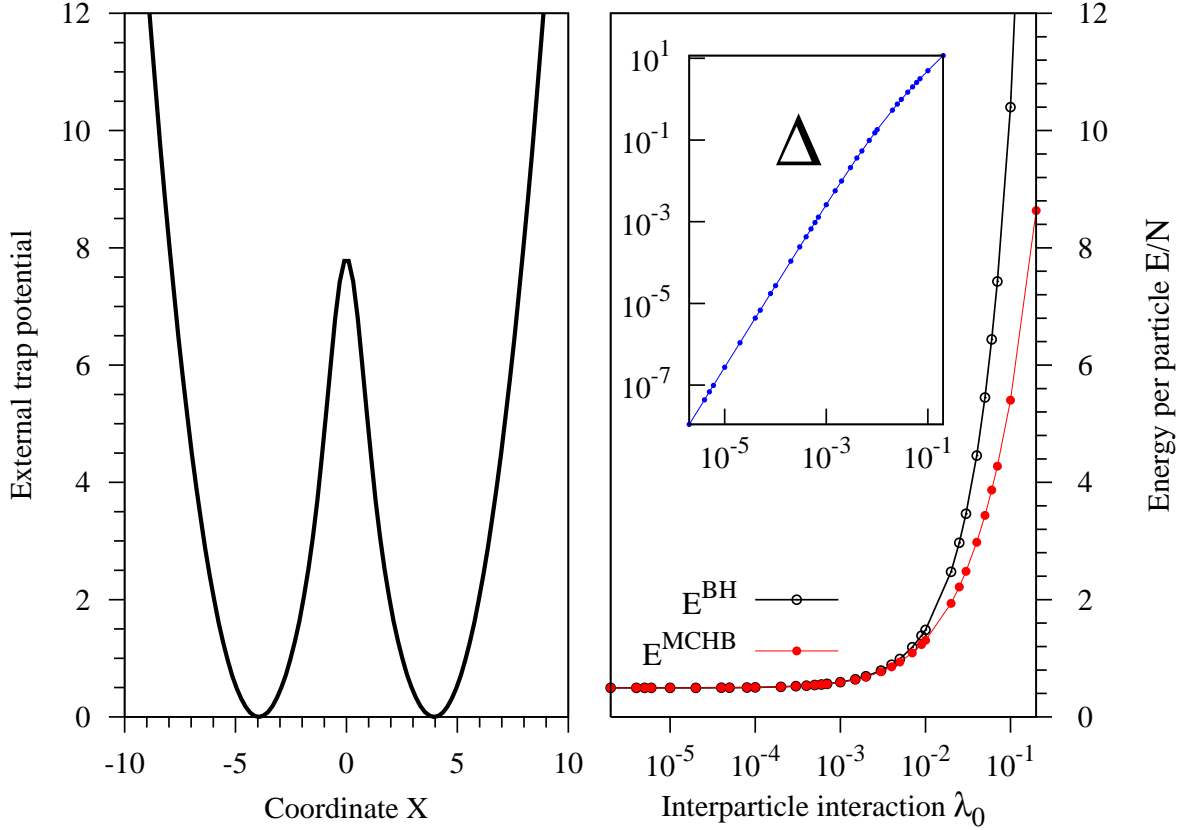


FIG. 1: (Color online) Right panel: The many-body energies per particle of the system of $N=1000$ trapped bosons as a function of inter-particle interaction strength λ_0 obtained within many-body basis sets constructed on fixed (black) and self-consistent (red) orbitals. As the fixed orbitals we use the eigenfunctions of the bare Hamiltonian (BH) with potential plotted on left panel. The self-consistent orbitals have been obtained within the framework of the MCHB(2) method. To demonstrate better the impact of self-consistency on the ground state energy we plot as Δ the difference between both energy curves in the inset. Left panel: Geometry of the symmetric one-dimensional trap used, see Eq.(40). It can be viewed as a combination of two harmonic traps separated by a barrier, see text for details.

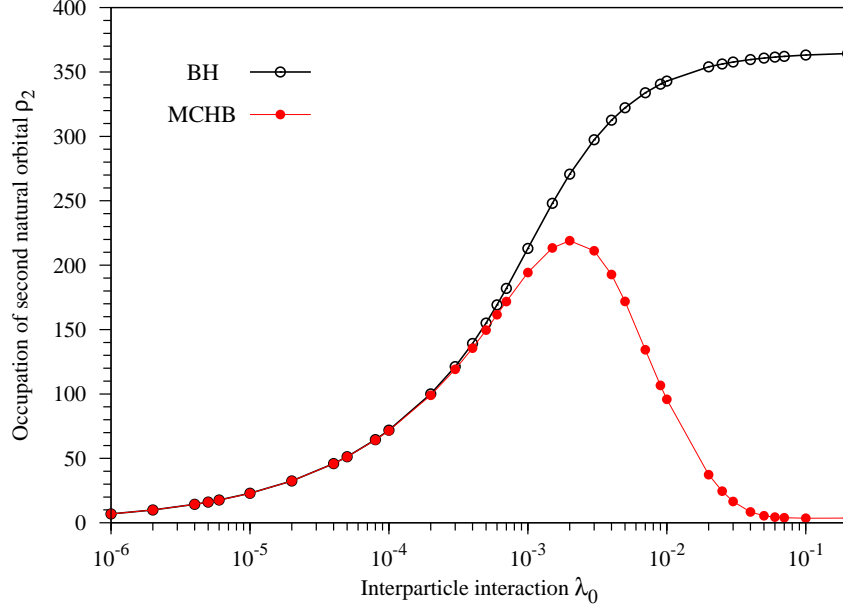


FIG. 2: (Color online) Demonstration that a lack of self-consistency can have a drastic impact on predicted many-body properties of the ground state. Fragmentation is plotted as a function of the inter-particle interaction strength. Shown is the fragmentation of $N = 1000$ bosons in the symmetric double-well potential of Fig.1. The occupation number $\rho_2 = N - \rho_1$ of the second natural orbital of the reduced one-particle density is plotted as a function of λ_0 . The solid (red) line with filled circles and the solid (black) line with open circles mark the self-consistent (MCHB) and fixed-orbital (BH) results, respectively.

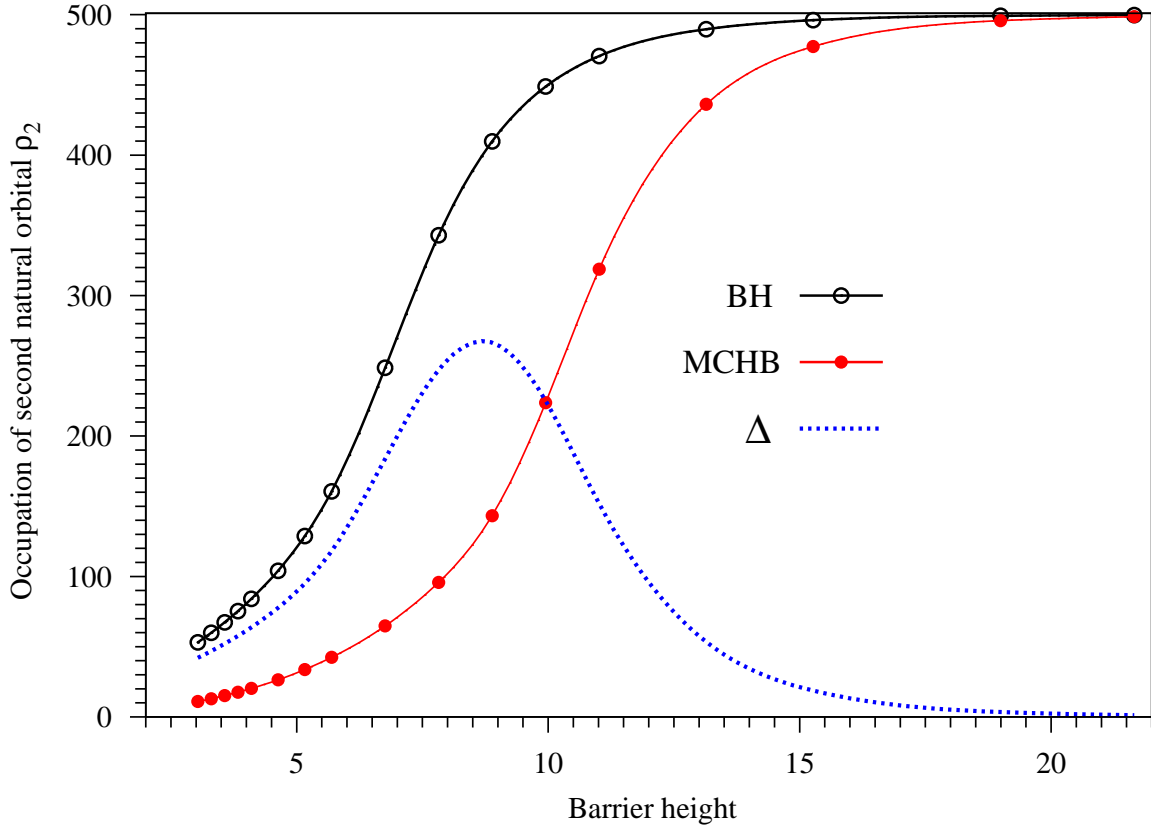


FIG. 3: (Color online) Fragmentation as a function of barrier height. The occupation number $\rho_2 = N - \rho_1$ of the second natural orbital of the reduced one-particle density is plotted as a function of the barrier height for $N=1000$ bosons trapped in a symmetric double-well potential (see text). The solid (red) line with filled circles and the solid (black) line with open circles represent the self-consistent (MCHB) and fixed-orbital (BH) many-body results, respectively. To emphasize the "non-trivial" difference between self-consistent and fixed-orbital results, the difference between both curves is plotted as a dashed (blue) line. The level of $\sim 25\%$ of fragmentation is achieved at barrier height of $V_{symm}(0) \approx 6.5$ units with fixed-orbital many-body method while self-consistency shifts this point to a barrier height $V_{symm}(0) \approx 10.5$ units, see text for discussion.

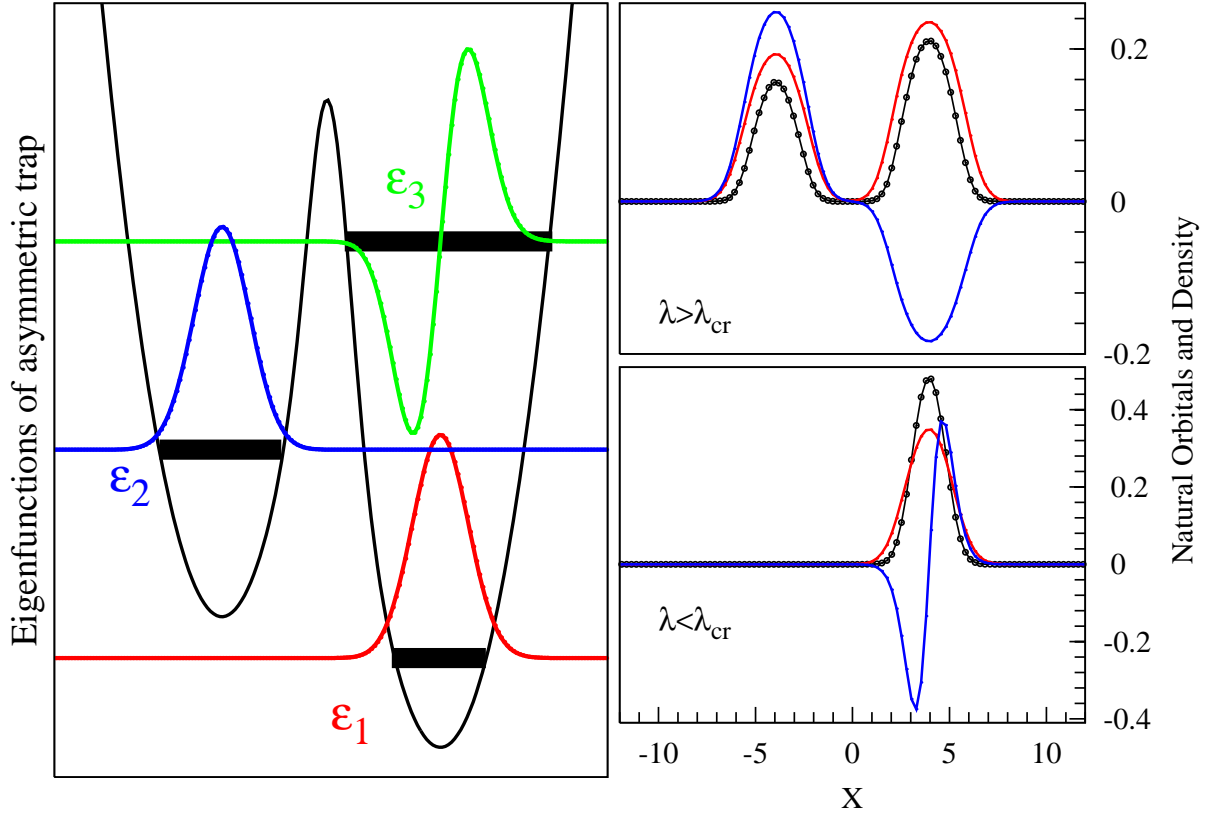


FIG. 4: (Color online) Study of $N=1000$ bosons in an asymmetric double-well using the MCHB(2) method. The asymmetric double-well potential and three eigenfunctions of the respective bare Hamiltonians lowest in energy are schematically shown in the left panel. Depending on the inter-particle interaction strength λ_0 the ground state of the system can enter two different regimes. For $\lambda < \lambda_0^{cr}$ the self-consistent MCHB(2) orbitals (solid lines) and respective normalized density (solid line with filled circles) are localized in the deeper well as depicted in the right lower panel. In the right upper panel it is shown that for $\lambda_0 > \lambda_0^{cr}$ the MCHB(2) natural orbitals are distributed over both wells.

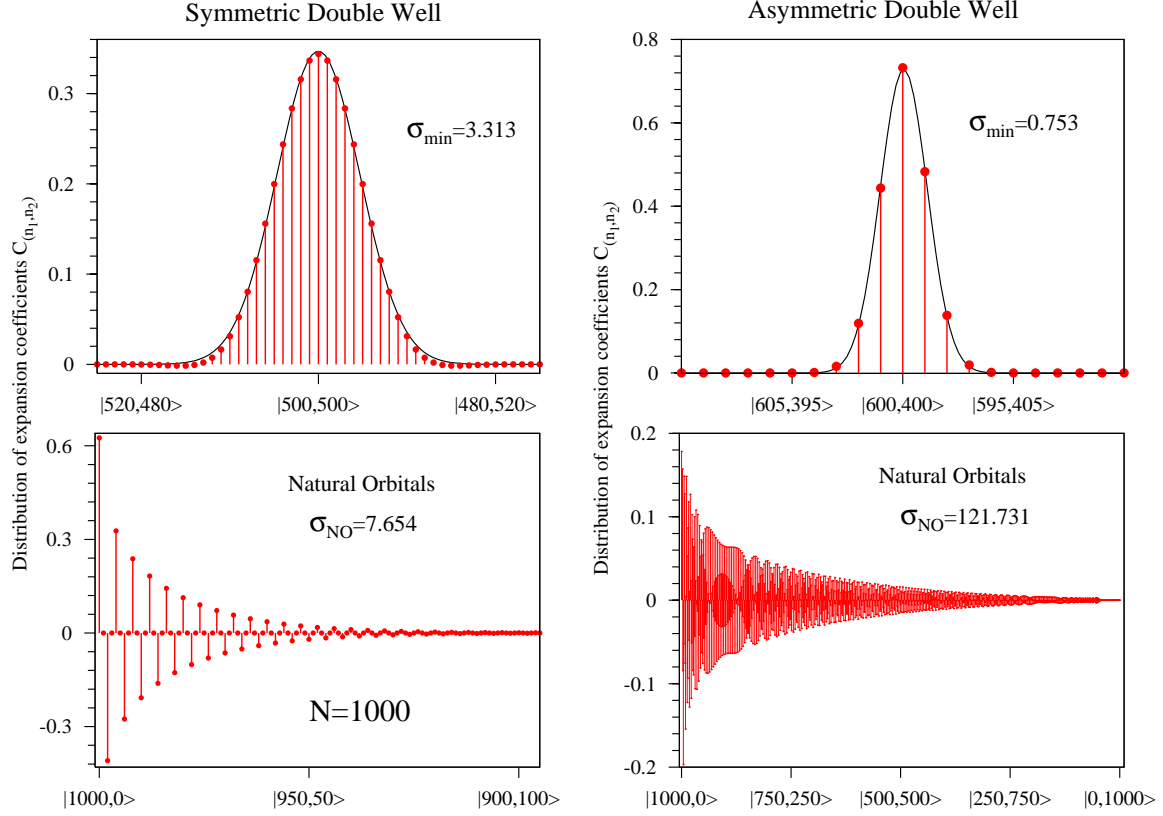


FIG. 5: (Color online) The distribution of the ground state expansion coefficients $C_{(n_1, n_2)}$ obtained in MCHB(2) depends on the particular choice of the one-particle basis functions. The left panels show the results for $N=1000$ bosons trapped in a symmetric double-well ($\lambda_0 = 0.01$). The right panels show the analogous results for the bosons in an asymmetric double-well ($\lambda_0 = 0.01$). Lower panels refer to the case where natural orbitals are used to construct the many-body basis functions $|n_1, n_2\rangle$. The width of a distribution is characterized in terms of its variance $\sigma_{n_1}^2 = \langle \hat{n}_1^2 \rangle - \langle \hat{n}_1 \rangle^2$. By applying unitary transformations (rotations) on the natural orbitals, the width of the distributions of the expansion coefficients can be minimized. Upper panels show the obtained distributions of the expansion coefficients with the minimal widths. The minimal distributions in these systems are well approximated by continuous Gaussian functions $[\frac{1}{\sigma_{min} \sqrt{2\pi}} \exp \frac{-(\xi - \langle n_1 \rangle)^2}{2\sigma_{min}^2}]^{1/2}$ plotted by black solid lines, see text for details.

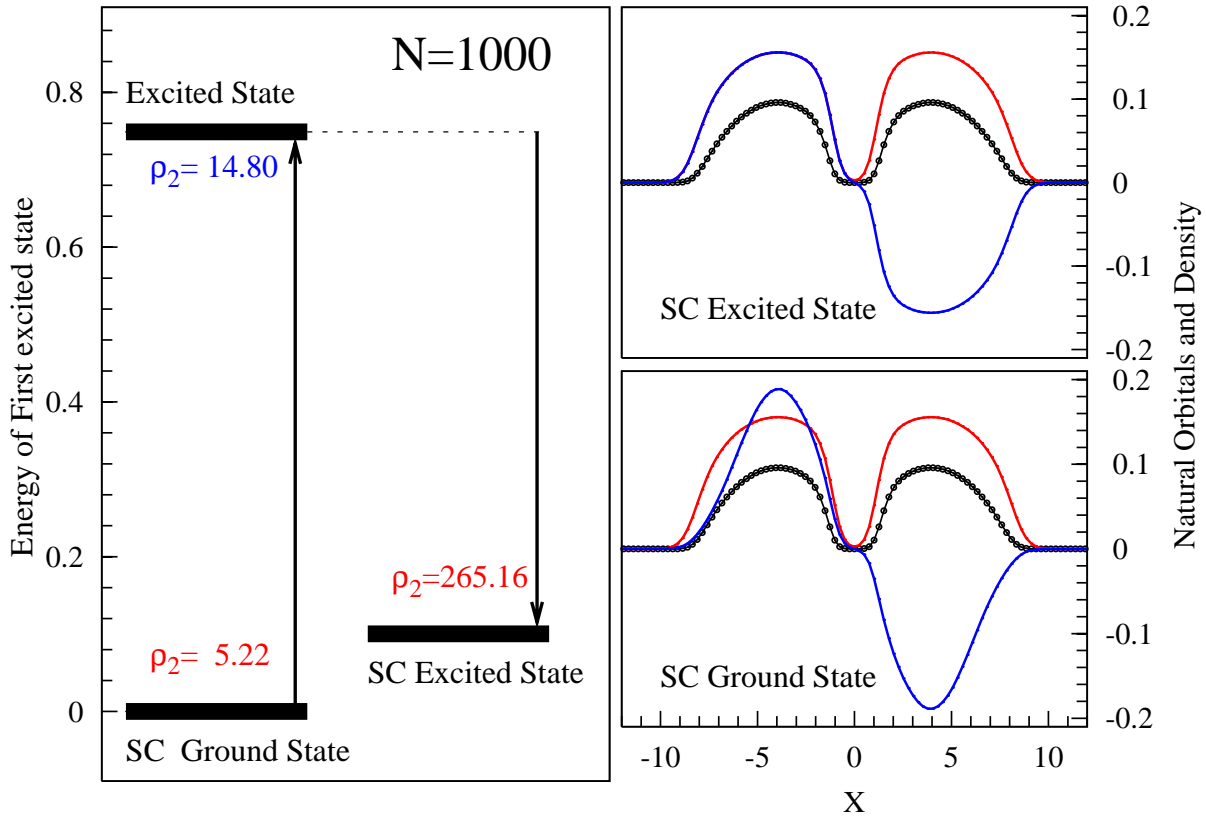


FIG. 6: (Color online) Demonstration that self-consistency can have a great impact on predicted many-body properties of excited states. Shown are results for $N=1000$ bosons trapped in a symmetric double well potential (see text for details). Left panel: Energy levels of the ground and first excited states obtained self-consistently are labelled as "SC Ground State" and "SC Excited State", respectively. For comparison we present the energy level of the non-self-consistent first excited state labelled as "Excited state", obtained by using the optimized ground state orbitals. The occupation of the second natural orbital ρ_2 ($\rho_1 = N - \rho_2$) is indicated for each state. Right panel: the MCHB solutions (natural orbitals) of the self-consistent ground and excited states (solid lines). The respective normalized densities are plotted by solid lines with filled circles.

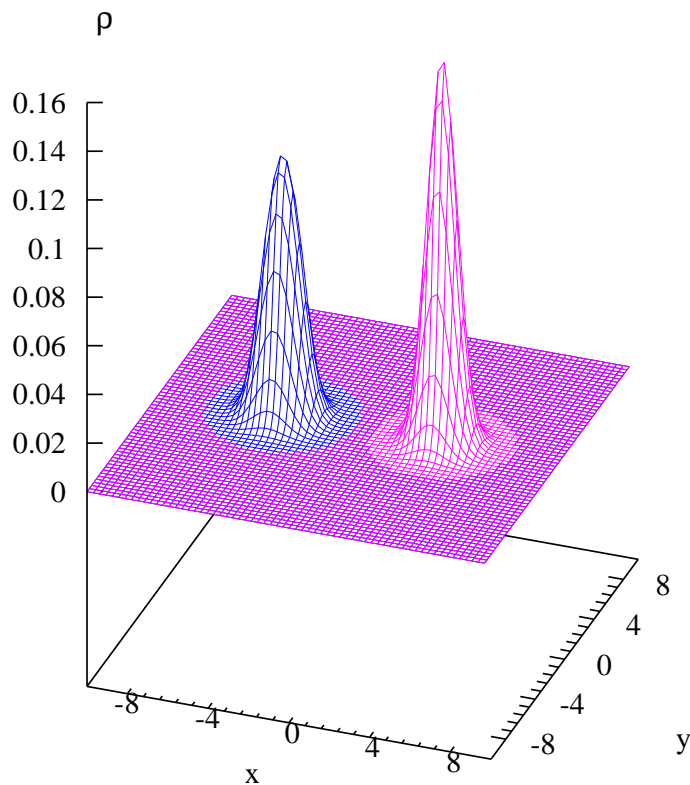


FIG. 7: (Color online) Illustration of the relevance of self-consistency for many-body treatments of bosonic systems in two-dimensions. Ground state density of $N=1000$ bosons at $\lambda_0 = 0.01$ in the symmetric two-dimensional double-well trap of Eq.(50). Due to the perfect symmetry of the trap potential, the total density consists of two equivalent parts each localized in one well. To highlight the difference, the part of the self-consistent MCHB(2) ground state density localized in the left well is plotted together with the part of the total density obtained with the fixed-orbital many-body method localized in the right well.

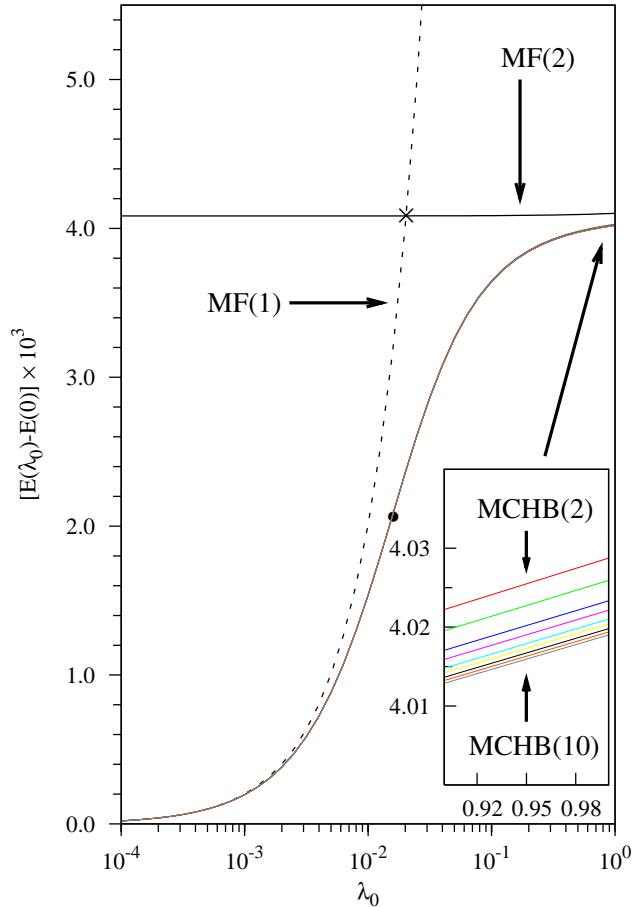


FIG. 8: (Color online) The total ground state energy of two bosons trapped in a symmetric double-well potential as a function of the inter-particle interaction strength λ_0 . All energies are plotted with respect to the ground state energy $E(0)$ of the non-interacting system. The energy curves obtained within the framework of the two-orbital MCHB(2) and multi-orbital MCHB(M) $M=3, \dots, 10$ are very close to each other. To distinguish between these curves we enlarge the scale 100 times in the inset. To emphasize the role of many-body effects we also show the results obtained using the one-orbital MF(1) (Gross-Pitaevskii) and two-orbital MF(2) mean-fields. The cross marks the transition point between "condensation" and "fragmentation" defined as the intersection of the MF(1) and MF(2) energy curves. At the MCHB(M) level we observe a smooth development from "condensation" to "fragmentation" instead of the sharp transition; the filled circle marks the respective transition point.